4-2014

Transport and Catabolism of Inositol Isomers in Sinorhizobium meliloti

Ee Leng Choong
Western Michigan University

Transport and Catabolism of Inositol Isomers in *Sinorhizobium meliloti*

by

Ee Leng Choong

A thesis submitted to the Graduate College
in partial fulfillment of the requirements
for the Degree of Master of Science
Biological Sciences
Western Michigan University
April 2014

Thesis Committee:

Silvia Rossbach, Ph.D., Chair
John Geiser, Ph.D.
Yan Lu, Ph.D.

Transport and Catabolism of Inositol Isomers in *Sinorhizobium meliloti*

Ee Leng Choong, M.S.

Western Michigan University, 2014

The nitrogen fixing symbiont of alfalfa, *Sinorhizobium meliloti,* is able to use inositols as the sole carbon source. In this thesis, the role of two genetic loci in *S. meliloti* was investigated; the first is involved in the transport of inositols and the second genetic locus is essential for the catabolism of D-*chiro*-inositol stereoisomers. The *S. meliloti ibpA* gene had been earlier described as playing a role in inositol transport, but this study identified the *SMb20072* gene product, called IbpB, as a second periplasmic binding protein involved in inositol transport. A single *ibpB* mutant and a double mutant *ibpAibpB* were constructed. The growth of the *ibpB* mutant was reduced as compared to the wild type when *myo*-inositol, D-*chiro*-inositol or pinitol were provided as sole carbon source, whereas the *ibpAibpB* double mutant did not grow at all. In addition, a mutant containing a kanamycin cassette in the *ioll*-like *SMb20711* gene was constructed to characterize its phenotype. The *SMb20711* mutant did not grow when D-*chiro*-inositol was provided as the sole carbon source. Also, the growth of the *SMb20711* mutant was impaired when it was grown with *myo*-inositol or pinitol as the sole carbon source as compared to the wild type. These results suggest that the *SMb20711* gene is essential for D-*chiro*-inositol catabolism and was called *ioll.*

ACKNOWLEDGEMENTS

I would like to thank my supervisor Dr. Silvia Rossbach for her guidance and support. I would also like to thank my thesis committee member Dr. John Geiser and Dr. Yan Lu who have taken great interest in my research. I am grateful to many of my friends and colleagues especially Mary Thwaites, and Drs. Petra Kohler, Vanessa Ravindran and Miles Roger who have assisted me in numerous ways throughout my graduate career at Western Michigan University. I would like to thank Dr. Anke Becker for providing the *S. meliloti* 2011 mTn*5*-STM mutants. My deepest gratitude goes to my parents for their unwavering support and encouragement. Finally, I would like to thank the Department of Biological Sciences and the Western Michigan University Graduate College. This work would not have been possible without the funding awarded to me, for which I am very grateful.

Ee Leng Choong

TABLE OF CONTENTS

Table of Contents - Continued

Table of Contents - Continued

LIST OF TABLES

LIST OF FIGURES

List of Figures - Continued

CHAPTER 1

INTRODUCTION

Nitrogen fixation

Nitrogen is the most abundant element in the atmosphere. Most atmospheric nitrogen is in a form that is unavailable to plants because it is chemically inert, exhibiting a strong triple bond between the two nitrogen atoms (Cheng, 2008). The process of nitrogen fixation can be divided into non-biological and biological nitrogen fixation. The non-biological nitrogen fixation comprises mainly industrial nitrogen fixation. The process of biological nitrogen fixation occurs in soil and water and is carried out by bacteria. Nitrogen-fixing bacteria can be found either free-living or in association with plants. Free-living nitrogen-fixing bacteria such as *Klebsiella* and *Azotobacter* are present in the soil. These bacteria are capable of fixing atmospheric nitrogen into ammonia via the enzyme nitrogenase. The symbiotic nitrogen-fixing bacteria such as *Rhizobium, Sinorhizobium* and *Bradyrhizobium* form an intimate relationship with legume plants. These bacteria infect legume plants non-parasitically and participate in a mutualistic relationship with the plants (Long, 1996). This relationship is important in fulfilling the nitrogen requirements for legume plants, which include soybeans, peas, and alfalfa.

Symbiotic nitrogen fixation by *Rhizobia*

The interaction of rhizobia with their host plants occurs in the soil around the roots of legume plants known as rhizosphere. The rhizosphere is rich in plant exudates such as amino acids, phenolic compounds, sugars, and other secondary metabolites (Jones et al., 2007). Rhizobium-legume interactions begin with the exchange of signals between plant and microbe. The process of nodulation starts with the roots of the legume plants exuding flavonoids into the rhizosphere. Flavonoids are metabolites that are able to chemically attract rhizobia (Jones et al., 2007). Rhizobia sense the flavonoids and respond to them by transcribing *nod* genes that encode genes for the synthesis of Nod-factors. Nod-factors are signaling molecules that are produced by bacteria during the initiation of nodules on the root of legumes. Structurally, Nod-factors are lipo-chito-oligosaccharides (LCOs) that induce multiple responses in the host plants such as changes in host gene expression and cell growth (Ehrhardt et al., 1996). The Nod factors stimulate one of the first responses in plant roots, which include a rise in calcium level and inner cortical cell division that eventually leads to the formation of a nodule primordium that then develops into a mature nodule. Nod factors also cause the plant root hair to deform and trap the bacterial cells that are associated with it. After the root hairs curl around the bacteria, and the plant root hair walls are degraded by hydrolysis, rhizobia will then enter the roots and an infection thread is formed (Newcomb et al., 1979). The bacteria divide and move along the infection thread towards the nodule primodia (Vandenbosch et al., 1985). Rhizobia are released from the infection threads into the plant cells and differentiate into bacteroids. The peribacteroid

membrane (PBM), which is derived from plant materials, encloses the bacteroids (Brewin et al., 1985). The PBM is thought to be responsible for regulating the nutrient flow between plant and bacteroids. The PBM also functions as an oxygen diffusion barrier. In the nodule, the concentration of oxygen is very low accommodating the oxygen sensitivity of nitrogenase, the nitrogen-fixing enzyme. Low oxygen concentration is the major signal controlling the expression of the *nif* genes that are responsible for bacteroids development as well as nitrogen fixation.

Nitrogen fixation is a very energy costly process. The bacteria will have to generate a large amount ATP in order to fix nitrogen. Therefore, the bacteria will require oxygen for respiration. Leghemoglobin is a hemoprotein found in the nitrogen-fixing root nodules of leguminous plants. It is an oxygen carrier that binds oxygen and transports it to the bacteroids in order to satisfy the respiratory needs of the bacteroids in the root nodules. Leghemoglobin has an extremely high affinity for oxygen, thus allowing the oxygen concentration in the nodule to be low enough for the nitrogenase to function but also high enough to provide oxygen to the respiring bacteroids.

Inositols

Inositols are sugar alcohols that exist as nine possible stereoisomers (Fig. 1). The major naturally occurring isomers are *myo-*, D-*chiro-*, L-*chiro-*, *scyllo-*, *muco-*, and *neo*-inositol. The *epi-*, *cis-*, and *allo*-inositol isomers are synthetic inositols. Some of the many soluble compounds that *Sinorhizobium* can utilize as the sole carbon source are *myo-*, D-*chiro-*, and *scyllo*-inositol (Kohler et al., 2010). *myo*-Inositol is the most abundant form of inositol that can be found in the rhizosphere and soil due to the degradation of organic matter.

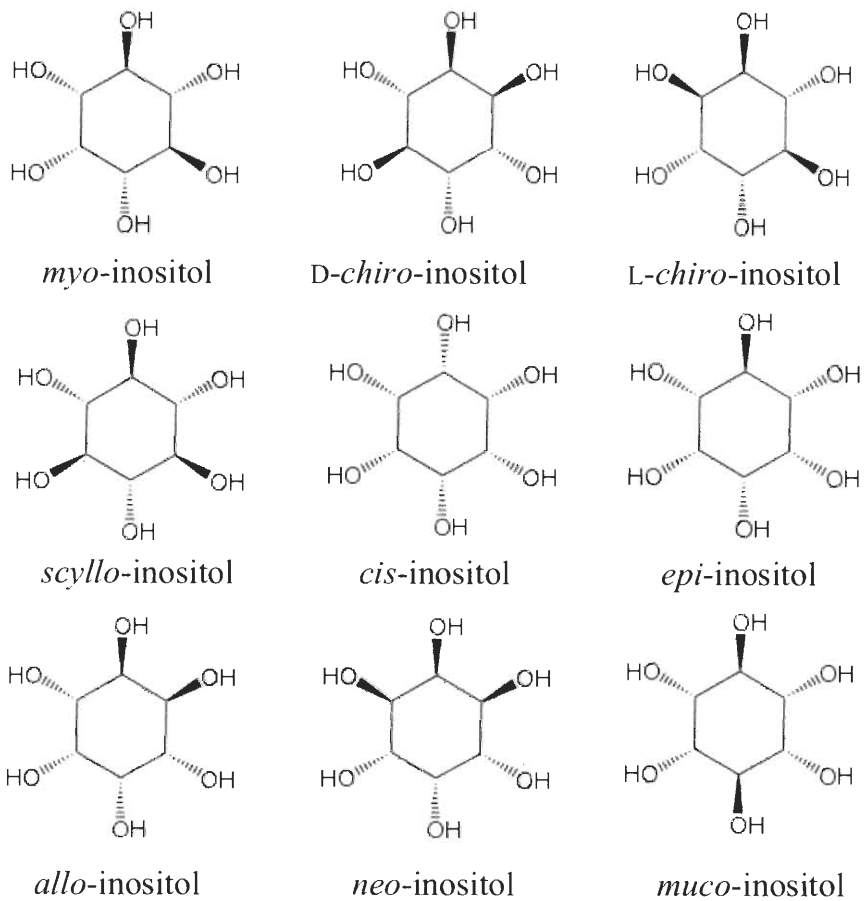

Figure 1: Structures of all nine inositol stereoisomers of inositol.

Inositols in eukaryotes

Inositols play an important role in mammalian systems. *myo*-Inositol has been shown to be a component of inositol phosphoglycan (IPG) molecules in mammals. These IPGs are cell membrane associated and serve as putative insulin secondary messenger (Valera-Neito et al., 1996). In respond to insulin, IPGs are released from glycosylphosphatidylinositols in the cell membranes into the cytoplasm, where they affect some of the enzymes implicated in insulin activity.

Especially D-*chiro*-inositol is known as an important second messenger in insulin signal transduction (Larner et al., 2010). In addition, D-*chiro*-inositol has been found to be an effective treatment for polycystic ovary syndrome (Larner et al., 2010). In this specific study, women with polycystic ovary syndrome who received D-*chiro*-inositol experienced some significant benefits such as lowered blood pressure, increased insulin sensitivity and a corresponding improvement in glucose disposal. Therefore, D-*chiro*-inositol has a great potential for the development of type II diabetes therapy (Yoshida et al., 2006).

scyllo-Inositol is another stereoisomer of inositol. Mammalian tissues contain less *scyllo*-inositol than *myo*-inositol. In contrast to *myo*-inositol and D-*chiro*-inositol, *scyllo*-inositol does not seem to be metabolized by the mammalian system. Nevertheless, it might have a function in the nervous system. Researchers at the University of Toronto have found that *scyllo*-inositol is able to block the development of amyloid-beta plaques in the brain of transgenic mice, which serve as

a model system for Alzheimer disease (Fenili et al., 2007). Therefore *scyllo*-inositol has a great potential in Alzheimer's disease therapy.

Also methylated inositols occur naturally in the environment. Pinitol, which is a methylated derivative of D-*chiro*-inositol and is found abundantly in legumes such as soybeans. Pinitol is one of the compatible solutes that are formed in plants as a response to salt or water stress (Bray et al., 1997). In recent years, pinitol has been used in laboratory and clinical trials as insulin sensitizer (Larner et al., 2010). One study was done on diabetic rats. Some of the rats were fed glucose alone or glucose supplemented with pinitol. The result indicated that rats that were fed with glucose supplemented with pinitol had lower blood glucose levels among all the diabetic rats (Larner et al., 2010). Pinitol was also tested in clinical trials that involved type II diabetes patients, who had previously responded poorly to the treatment with other hypoglycemic drugs (Kim et al., 2007). When the patients' diets were supplemented with pinitol, their blood glucose levels were lowered significantly (Kim et al., 2005; 2007).

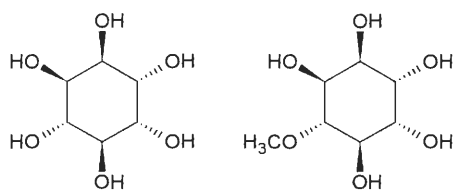

D-*chiro*-inositol Pinitol

Figure 2: Structures of D-*chiro*-inositol and its methylated form, pinitol.

Inositols in prokaryotes

Unlike eukaryotes, in Bacteria and Archaea, inositol-containing molecules are not ubiquitously found but restricted to certain classes of prokaryotes. Inositol solutes involved in osmotic balance have been detected in hyperthermophilic Archaea (Martin et al., 1999). Inositol-phosphodiesters are used by hyperthermophilic Archaea for protection against high temperature (Borges et al., 2006). Some bacteria of the phylum *Actinobacteria* are able to use inositols in their cellular processes as well (Michell, 2008). Nonetheless, the transport and metabolism of inositols has been best studied in bacteria such as *Firmicutes* and *Proteobacteria*. Inositols can serve as sole carbon and energy source for some soil bacteria including *Klebsiella aerogenes, Pseudomonas putida, Bacillus subtilis, Caulobacter crescentus,* and *S. meliloti.*

Early studies of inositol transport and catabolism in bacteria

The genes necessary for transport and to catabolize inositols have been characterized in some bacterial species; the investigation of *myo*-inositol has made notable progress in the last three decades. Early studies on inositol transport and catabolism systems have been carried out in *K. aerogenes, P. putida, Salmonella enterica* serovar typhimurium, *C. crescentus* and *B. subtilis.* These studies mainly focused on *myo*-inositol.

The γ-proteobacterium *K. aerogenes* was used as the model organism in the biochemical research of *myo*-inositol degradation. Magasanik's group described the enzymes that were involved in the degradation of *myo*-inositol by performing

enzyme assays and kinetic studies. Magasanik's group was not able to explain the complete inositol catabolism pathway in detail, but established a basis for investigating *myo*-inositol catabolism by characterizing the enzymes and describing the possible intermediates in the pathway of *K. aerogenes* (Berman et al., 1966a and 1966b; Anderson et al., 1971a and 1971b).

The main model organism for inositol catabolism that has been studied recently is the Gram-positive soil bacterium *B. subtilis* that belongs to the *Firmicutes* phylum. The studies of the inositol catabolism in *B. subtilis* were conducted by Yoshida et al. (1997, 2008) who characterized the *iol* operon that is responsible for *myo*-inositol catabolism. The researchers found that the *iol* cluster consists of ten *iol* genes, *iolABCDEFGHIJ*, the function of which is shown in Fig. 3. The gene products of the *iol* genes are involved in *myo*-inositol catabolism, as disruption of each gene individually caused the bacteria to lose the ability to degrade *myo*-inositol (Yoshida et al., 1997).

A.

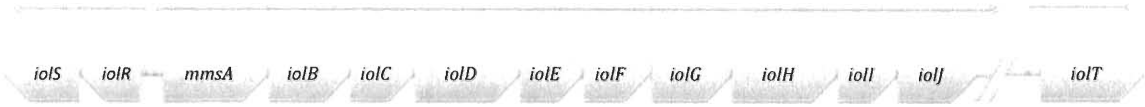

B.

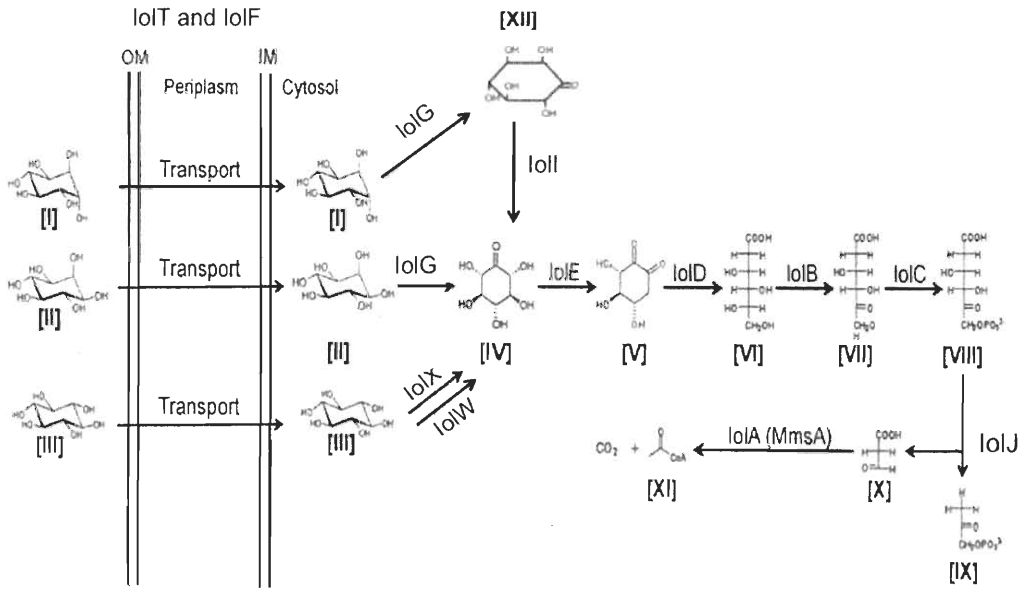

Figure 3: Organization of the inositol (*iol)* catabolism genes (A) and the inositol catabolism pathway of *B. subtilis* (B). Compounds: D-*chiro*-inositol [I]; *myo*-inositol [II]; *scyllo*-inositol [III]; 2-keto-*myo*-inositol [IV]; 3D- (3,5/4)-trihydroxycyclohexane-1,2-dione [V] 5-deoxy-D-glucuronic acid [VI]; 2-deoxy-5-keto-d-gluconic acid [VII]; 2-deoxy-5-keto-d-gluconic acid 6-phosphate [VIII]; dihydroxyacetone phosphate [IX]; malonate semialdehyde (MSA) [X]; acetyl coenzyme A [XI]; 1-keto-*D-chiro*-inositol [XII]. Enzymes: IolG, *myo*-inositol dehydrogenase; IolI, 1-keto-D-*chiro*-inositol isomerase; IolE, 2KMI dehydratase; IolD, 3-d-(3,5/4)-trihydroxy-cyclohexane-1,2-dione hydrolase; IolB, 5-deoxy-glucuronate isomerase; IolC, 2-deoxy-5-keto-d-gluconic acid kinase; IolJ, aldolase; IolA, methylmalonate semialdehyde dehydrogenase; IolT, IolF, inositol transporters; IolX, IolW, *scyllo*-inositol dehydrogenases (Modified after Yoshida et al. 1997, 2002, 2008, and 2010).

The *iolG* gene encodes the first enzyme in the inositol catabolism pathway, the NAD^+ dependent *myo*-inositol dehydrogenase, which carries out the initial oxidation of *myo*-inositol to its corresponding ketone, 2-keto-*myo*-inositol. In the second step, 2-keto-*myo*-inositol is converted into 3D-(3,5/4)-trihydroxy-cyclohexane-1,2-dione via the *iolE* product, 2-keto-*myo*-inositol dehydratase. 3D-(3,5/4)-trihydroxy-cyclohexane-1,2-dione is the substrate for the hydrolase IolD, which is the third enzyme in the inositol catabolism pathway, generating 5-deoxy-D-glucuronic acid. In the fourth step, 5-deoxy-D-glucuronic acid is isomerized into 2-deoxy-5-keto-D-gluconic acid by the isomerase IolB. After this step, the IolC kinase phosphorylates 2-deoxy-5-keto-D-gluconic acid resulting in 2-deoxy-5-keto-D-gluconic acid 6-phosphate (KDGP). In the fifth step of the inositol catabolism pathway, KDGP is being cleaved into dihydroxyacetone phosphate and malonic semialdehyde by the aldolase IolJ. Last but not least, malonic semialdehyde is converted into acetyl-CoA and carbon dioxide by the *iolA* gene product. The *iolA* gene was later named *mmsA,* based on the name of its protein product, methylmalonate semialdehyde dehydrogenase.

B. subtilis does not only use *myo*-inositol but also D-*chiro*- and *scyllo*-inositol as the sole carbon source. In *B. subtilis*, D-*chiro*-inositol is initially oxidized to 1-keto-*chiro*-inositol by the *myo*-inositol dehydrogenase (Fig. 3). After the oxidation, the *iolI* gene product, an inosose isomerase, will convert the resulting 1-keto-*chiro*-inositol into 2-keto-*myo*-inositol (2KMI). 2KMI will then be further catabolized by the other enzymes of the *myo*-inositol pathway. The initial oxidation of *scyllo*-inositol requires a different oxidoreductase, because the *myo*-inositol

dehydrogenase cannot utilize *scyllo*-inositol as a substrate (Freese at al., 1979). *B. subtilis* possesses two *scyllo*-inositol dehydrogenases that are encoded by *iolX* and *iolW*. Both enzymes probably convert *scyllo*-inositol into 2-keto-*myo*-inositol, which is further broken down by the other *iol* gene products. Interestingly, studies have shown that only IolX is essential for the growth with *scyllo*-inositol as the sole carbon source (Morinaga et al., 2010).

The *iolRS* operon is located upstream of the *iol* operon, which is transcribed from another inositol-inducible promoter divergently to the *iol* operon. The repressor encoded by *iolR* is responsible for the regulation of all the *iol* genes as well as the *iolRS* operon (Yoshida et al., 1997, 1999). As the *iol* and *iolRS* operons are divergently transcribed, they constitute the *iol* divergon. In the absence of *myo*-inositol, the *iolR* gene product binds to the operator site within the two *iol* promoter regions to repress the transcription. However, when *myo*-inositol is present, the catabolic intermediate 2-deoxy-5-keto-D-gluconic acid 6-phosphate acts as the inducer that will bind IolR and cause the repressor to fall off from its target operator. The *iolS* gene in the *iolRS* operon encodes an aldo/keto reductase. So far, no function was suggested for the IolS protein in inositol catabolism. Yoshida et al. (1997) suggested that the *iolS* gene might not be necessary for inositol catabolism, because disruption of the *iolS* gene affected neither growth with inositol nor the inducibility and catabolite repression of the *myo*-inositol dehydrogenase gene.

Other studies have been conducted focusing on *myo*-inositol catabolism in the plant symbiotic α-proteobacteria *Rhizobium leguminosarum, Sinorhizobium*

fredii, and *S. meliloti.* The *myo*-inositol dehydrogenase was characterized in *R. leguminosarum* bv. *viciae, S. fredii,* and *S. meliloti* (Poole et al., 1994, Jiang et al., 2001 and Galbraith et al., 1998). Also, the involvement of the *iolE* gene product, the 2-keto-*myo*-inositol dehydratase, in *myo*-inositol catabolism was shown for *R. leguminosarum* bv. *viciae* and *S. fredii* (Poole et al., 1994, and Yoshida et al., 2006).

myo-Inositol catabolism in *R. leguminosarum* was postulated to be similar as in *K. aerogenes,* because the first two enzymes in the pathway, *myo*-inositol dehydrogenase and 2-keto-*myo*-inositol dehydratase both were shown to be inducible by *myo*-inositol (Poole et al., 1994). The researchers also suggested that *myo*-inositol catabolism plays an important role during the early stages of competition for nodule occupancy. This result was supported by an experiment conducted by Fry et al. (2001). When the *iolA* or *iolD* mutants of *R. leguminosarum* bv. *viciae* were inoculated onto plants individually, both mutants nodulated and fixed nitrogen as well as the wild type. Nevertheless, the *R. leguminosarum* bv. *viciae iolA* and *iolD* mutants were strongly impaired in their ability to compete with the wild type in a competition plant assay (Fry et al., 2001). In addition, it was found that the nitrogen fixing ability of bacteroids derived from an *S. fredii idhA* mutant was reduced (Jiang et al., 2001). These findings support the theory that these nitrogen-fixing symbionts require a functional inositol catabolic pathway for successfully competing during the host plant nodulation.

In contrast to the organization of the *iol* genes in *B. subtilis,* the inositol catabolism genes of *S. meliloti* are not arranged in a single cluster. In fact, the

genome of *S. meliloti* consists of three replicons, which are the chromosome, pSymA and pSymB megaplasmids. The *idhA* gene of *S. meliloti* is located on the pSymB plasmid, whereas most of the other *iol* genes are organized in one cluster on the chromosome (Fig. 4A). All *iol* genes are orientated in the same direction (Fig. 4A). Interestingly, the *iolA* gene is located further away from the rest of the genes on the chromosome. In *B. subtilis*, the IolR protein is a repressor of the DeoR-family of bacterial regulators. Its DNA-binding properties and regulatory function were studied by Yoshida et al. (1999). In contrast, the *S. meliloti* transcriptional regulator encoded by *iolR* belongs to the RpiR repressor family (Kohler et al., 2011).

A.

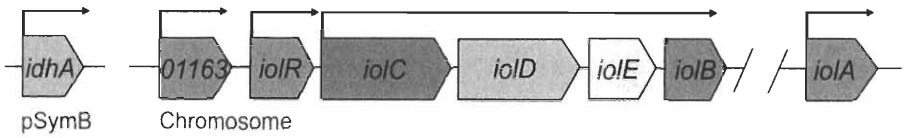

B.

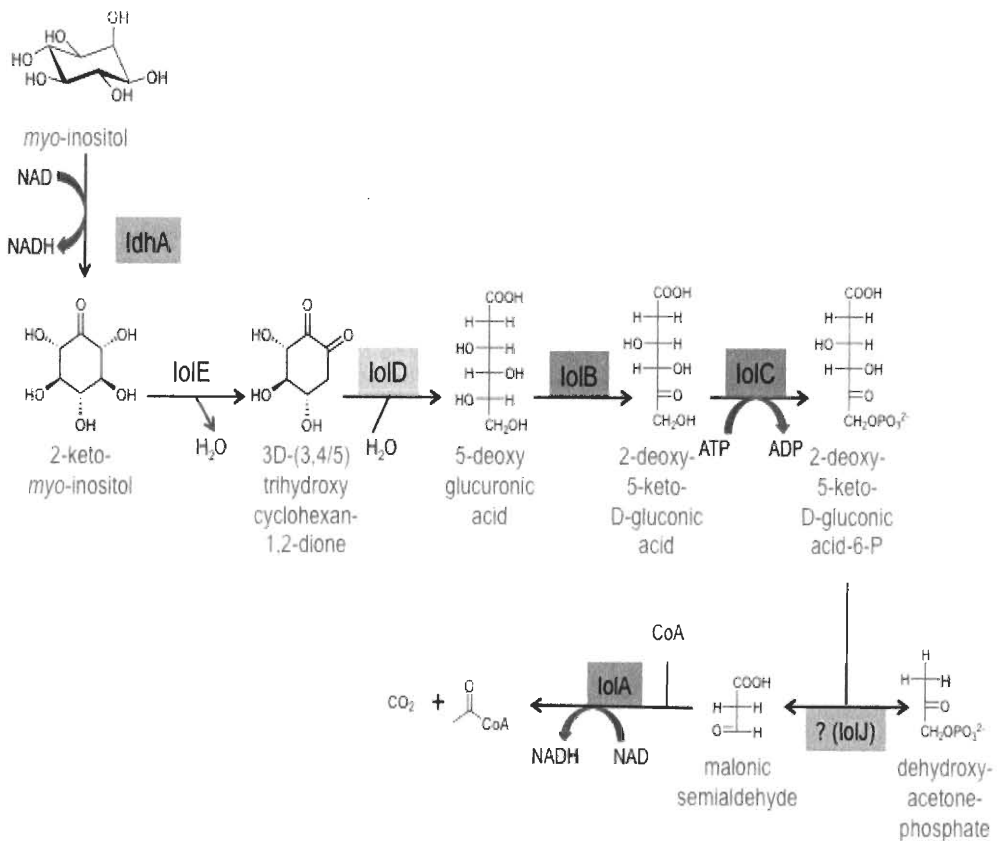

Figure 4: Organization of the *Sinorhizobium meliloti* inositol (*iol)* catabolism genes (A) and proposed inositol catabolism pathway in *S. meliloti* (B).

A complete study of the roles of the predicted gene products of the *iol* genes in the catabolism of different inositol stereoisomers has been conducted using mutants of *S. meliloti* 2011 that contained transposon insertions in the *idhA, iolA,* and each of the individual *iolCDEBR* genes (Kohler et al., 2010). The results obtained from the study showed that when grown in minimal media with *myo*-inositol as the sole carbon source, the wild type *S. meliloti* 2011 strain grew, while the corresponding *idhA, iolC, iolD, iolE, iolB,* and *iolA* mutants did not grow at all. Hence, this proves that the *idhA, iolCDEB,* and *iolA* are essential for *myo*-inositol catabolism in *S. meliloti* (Kohler et al., 2010) and their role is shown in Fig. 4B. Aside from *myo*-inositol, *S. meliloti* is also able to use D-*chiro*-inositol as the sole carbon source (Kohler et al., 2010), but an *iolI*-like gene, which was shown to be essential in *B. subtilis* for inositol catabolism has never been identified in *S. meliloti*. Also the dual role of the *iolA* gene is interesting to mention: it is not only essential for inositol catabolism, but it was also found to be essential for valine catabolism in *Pseudomonas spp.* (Bannerjee et al., 1970 and Steele et al., 1992) as well as in *S. meliloti* (Kohler et al., 2011).

Inositol transport

Although a lot of knowledge has been accumulated about inositol metabolism, not as much is known about inositol transport. Bacteria and Archaea live in diverse and often constantly changing environments where nutrients are usually very scarce. To be competitive in these niches, they have evolved active uptake systems that are able to scavenge low concentrations of nutrients efficiently. In general, transport systems in bacteria allow the uptake of essential nutrients and carbon sources such as inositols, as well as the excretion of cellular waste, and communication between cells and the surrounding environment. The two largest families of solute-specific transporters found in nature are the ATP binding cassette (ABC) family and the major facilitator superfamily (MFS).

The ATP-binding cassette (ABC) transporters are transmembrane proteins that harness the energy from ATP hydrolysis to carry out the transport of various substrates across membranes. ABC transporters consist of three components: a periplasmic binding protein, a transmembrane permease and a cytoplasmic ATPase.

The major facilitator superfamily (MFS) transporters are secondary carriers that are capable transporting small molecules using chemiosmotic ion gradients without using ATP. This type of transporter is present ubiquitously in Bacteria, Archaea, as well as Eukarya. They can function as symporters, uniporters, or antiporters.

Some new types of solute importers have also been recently identified in various bacterial genera and are called the tripartite tricarboxylate transporters

(TTT) (Winnen et al., 2003) and the tripartite ATP-independent periplasmic (TRAP) transporters (Fischer et al., 2010).

The TTT and TRAP transport systems are unique in the sense that they utilize a periplasmic binding protein in combination with a secondary transporter (Fischer et al., 2010). Both TRAP and TTT transport systems consist of three proteins: a periplasmic binding protein, a small and a large integral membrane protein of unequal size (Fig. 5). However, there is no significant sequence similarity between these two systems (Winnen et al., 2003).

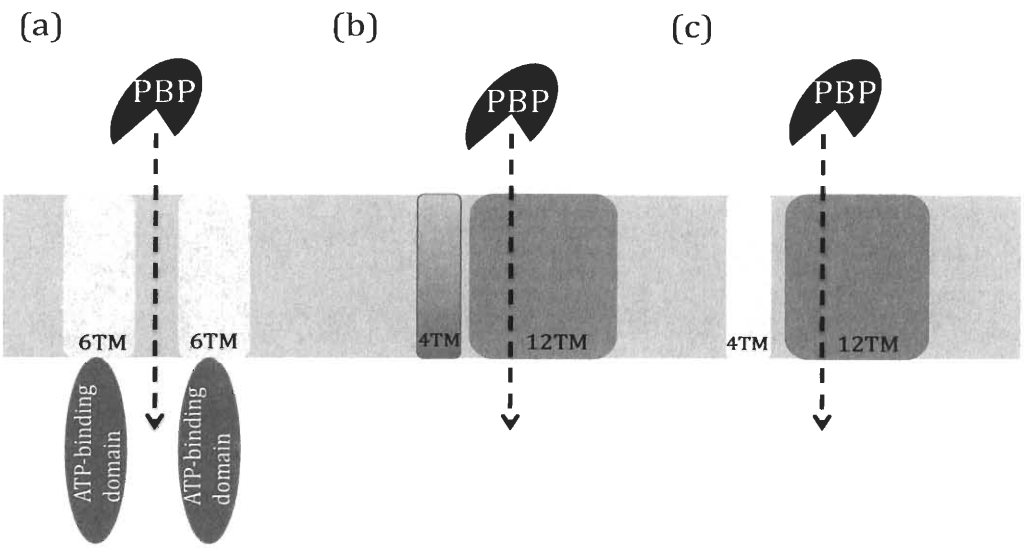

Figure 5: Comparison of the ABC, TTT, and TRAP transport systems that are associated with bacterial periplasmic binding proteins. (a) Organization of ABC transporters. The ABC transporters have two-membrane associated domains and two ATP-binding domains. (b) The TTT transporters have the same membrane protein organization (4-TM and 12-TM) as the TRAP transporter (c).

Various bacteria use these transport systems to transport carbon sources into the cells. Amongst these are *K. aerogenes, P. putida, S. enterica* serovar typhimurium, *C. crescentus* and *Rhizobiaceae*. The inositol transporters of these bacteria are described in detailed below.

Klebsiella aerogenes

The *K. aerogenes* system of inositol transport is unique due to the fact that the transporter facilitates the import of both *myo*- and *scyllo*-inositol (Deshusses et al., 1977). The inositol transporter of *K. aerogenes* that facilitates the import of both isomers is a proton symporter. The pH shift due to the proton uptake was specifically correlated with inositol transport, since a transport-linked pH increase was observed only with inositol-induced cells during the experiment. The rate of proton uptake was also enhanced in the presence of *scyllo*-inositol, which is consistent with simultaneous entry of inositols and protons during the active transport in *K. aerogenes*. Thus, the inositol transporter in *K. aerogenes* functions as a proton-inositol symport system that does not directly use ATP implicating that the MFS transport family is used rather than an ABC transport system.

Pseudomonas putida

The inositol transport system in *P. putida* seems to involve more than one protein. The unique feature of the *Pseudomonas* spp. transport system is the presence of a periplasmic binding protein that was not observed previously in *K. aerogenes* (Reber et al., 1977). A *myo*-inositol specific binding protein from *Pseudomonas* spp. was purified and characterized (Deshusses et al., 1984). From the kinetic data gathered, it was deduced that *P. putida* contains two transport systems for *myo*-inositol. Furthermore, the binding protein was shown to be responsible for high affinity transport (Reber et al., 1977). This was discovered by growing the bacterial cells to stationary phase, osmotically shocking them and then measuring the amount of inositol bound to periplasmic binding proteins that are now found in the supernatant. Osmotically shocked cells did not transport cyclitols at high affinity but retained a low affinity uptake activity. This implicated that one high and one low affinity transport system are present in *P. putida.* Therefore, the major inositol transport in *Pseudomonas* spp. is likely to be facilitated by a transporter that utilizes a periplasmic binding protein.

Bacillus subtilis

Two decades later, scientists discovered that the inositol transport in *Bacillus subtilis* is facilitated by the products of two genes, *iolT* and *iolF* (Yoshida et al., 2002). The IolT and IolF proteins show homology to the MFS superfamily. Mutants were constructed with individual in-frame deletions in both genes. When the *iolT* mutant was grown with *myo*-inositol as the sole carbon source, after 8 hours, the mutant reached an OD_{600} ≈0.8, which is lower than the wild-type strain. This indicated that the *iolT* mutant was impaired in utilizing *myo*-inositol as the sole carbon source. When the *iolF* knockout mutant was subjected to the same conditions, the single inactivation of *iolF* gene led to a less obvious growth defect on *myo*-inositol as compared to the *iolT* mutant. The *iolF* mutant reached an OD_{600} ≈2.3, which is comparable to the wild-type strain. This suggested that the *iolF* mutant was still capable of taking up *myo*-inositol even after the *iolF* gene was inactivated. When a double mutant with mutations in both *iolT* and *iolF* was tested, the phenotype for the double mutant was more drastic than the phenotype for the *iolT* mutant alone (Yoshida et al., 2002). The *iolF iolT* double mutant reached an OD_{600} ≈0.65, which indicated a more severe growth defect when both of the transport genes were inactivated. Therefore, it was concluded that *iolT* and *iolF* encode a major and a minor *myo*-inositol transporter in *B. subtilis,* respectively (Yoshida et al., 2002).

Salmonella enterica serovar typhimurium

The *myo*-inositol utilization genes of *S. enterica* serovar Typhimurium are located on a genomic island. The systematic knockout of the genes in the genomic island revealed that this island encodes all the enzymatic activities required for *myo*-inositol catabolism. The genes *iolR, iolB, iolA, iolE, iolG1, iolC1/2* and *iolD2* were found to be essential for utilizing *myo*-inositol. Upon deletion of these genes, the phenotypes showed that these mutants could not grow with *myo*-inositol as the sole carbon source (Kröger et al., 2009).

The *myo*-inositol transport system of *S. enterica* serovar typhimurium is very similar to the *B. subtilis* inositol transport system. In contrast, the organization of the genes encoding *myo*-inositol transport, regulations as well as catabolism are very different from the conserved module that is found in α-proteobacteria. Two *myo*-inositol transporters have been identified in *S. enterica,* which are encoded by *iolT1* and *iolT2* (Kröger et al., 2010). The role of both *myo*-inositol transporters was investigated by construction of in-frame-deletion mutants. The transcriptional activities of the two transporter genes were monitored using a luciferase reporter system. The luciferase reporter assays revealed IolR to be a repressor of *iolT1* and *iolT2* transcription (Kröger et al., 2010). It was also shown that the *myo*-inositol transporters in *S. enterica* serovar typhimurium indeed belonged to an MFS family that functions as proton symporter. The IolT1 and IolT2 were found to be the major and minor *myo*-inositol transporters in *S. enterica* serovar typhimurium, respectively (Kröger et al., 2010).

Caulobacter crescentus

myo-Inositol transport and catabolism genes in *C. crescentus* have been described by Boutte et al. (2008). The genes required for growth with *myo*-inositol as the sole carbon source are arranged in two clusters in *C. crescentus.* By computer analysis, the first cluster was identified to contain the *ibpA, iatA,* and *iatP* genes. These three genes were predicted to encode the periplasmic-binding protein, permease component and the ATP-binding cassette of an ABC transporter, respectively. The structural genes that are required for *myo*-inositol catabolism and the regulatory gene *iolR* are located within the second cluster. To confirm that the transporter *ibpA-iatA-iatP* operon in *C. crescentus* was necessary for growth in *myo*-inositol, mutants were constructed with insertions in these genes. *C. crescentus* transporter mutants were not able to grow using *myo*-inositol as the sole carbon source. The growth of the transporter mutant with *myo*-inositol was restored to the wild-type phenotype by complementation with a vector carrying the entire *ibpA-iatA-iatP* locus (Boutte et al., 2008).

Rhizobiaceae

Further computer analysis of the *ibpA, iatA,* and *iatP* genes in *C. crescentus* revealed high similarity to genes in other genera of the *α-Proteobacteria* phylum such as *Agrobacterium, Bradyrhizobium, Brucella, Mesorhizobium,* as well as *Sinorhizobium* (Boutte et al., 2008). In *S. meliloti*, the *SMb20712, SMb20713,* and *SMb20714* genes in *S. meliloti* revealed high similarity to the *ibpA, iatA, and iatP* genes of *C. crescentus.*

Growth studies were performed using the *S. meliloti ibpA* mutant (Pobigaylo et al. 2006), the results showed that the *ibpA* mutant was not able to grow using *myo*-inositol (Boutte et al., 2008). However, Thwaites (2013) used the same *S. meliloti ibpA* mutant to perform a growth study with *myo*-inositol, and the *ibpA* mutant had a delayed growth and was able to regain growth after three days. These data suggested that the *ibpA* gene product is involved in the initial transport of inositols but over time the inositols are entering the cells via some other alternative pathway (Thwaites, 2013).

To verify that the insertion in the *ibpA* gene was indeed responsible for the initial transport of inositols, a complementation experiment was performed. The wild-type *ibpA* gene was cloned into the broad-host range expression vector pTE3 and conjugated into the *ibpA* mutant (Thwaites, 2013). These data showed that the complemented mutant still showed a delayed growth indicating that the mini-*Tn5* insertion in the *ibpA* gene most likely had a polar effect on the *iatA* and *iatP* genes that are located downstream. Therefore, a larger fragment containing the *ibpA, iatA,*

and *iatP* genes was cloned into pTE3 vector, and conjugated into the *ibpA* mutant. When all three genes were cloned into the broad host range vector, the growth of the *ibpA* mutant was restored to the wild-type level (Thwaites, 2013).

Objectives

The main goal of this thesis is to carryout further investigations into the inositol transport and catabolism with *S. meliloti* as the model organism. When I first started my thesis work, there were three open questions concerning inositol transport and catabolism in *S. meliloti* that caught my attention.

1. Since the *ibpA* mutant regained growth after three days, is there a second transporter involved in the transport of inositols in *S. meliloti*?
2. Which gene is responsible for D-*chiro*-inositol catabolism in *S. meliloti*?
3. What is the role of the *iolA* gene and is the disruption of the *iolA* gene in the *iolA* mutant really the cause of its phenotype?

Concerning the first question: There are three genes in the *S. meliloti* genome *SMb20712, SMb20713* and *SMb20714,* which encode an ABC transporter involved in inositol transport. Interestingly, the *SMb20712* mutant was able to grow with *myo*-inositol as the sole carbon source after an initial delay. The hypothesis is that there is a second transporter involved in the transport of inositol compounds. Another gene encoding a periplasmic binding protein, *SMb20072,* was shown to be induced by *myo*-inositol (Mauchline et al., 2006). The hypothesis is that the *SMb20072* gene encodes a second periplasmic binding protein involved in inositol transport. To prove this hypothesis, a single mutant with an insertion in the *SMb20072* gene and a double mutant with an insertion in the *SMb20072* and *SMb20712* genes should be constructed to characterize the role of the second periplasmic binding protein in inositol transport of *S. meliloti*.

Concerning the second question: The Rossbach laboratory has previously characterized the genes necessary for *myo*-inositol catabolism as well as the transcriptional regulation of these genes in *S. meliloti* (Kohler et al., 2010; 2011). Nevertheless, an IolI like-gene that is responsible for D-*chiro*-inositol catabolism still remains unidentified in *S. meliloti*. The hypothesis is that the *SMb20711* gene of *S. meliloti*, which is annotated in the KEGG database as *iolI*-like, is indeed involved in D-*chiro*-inositol catabolism. A *SMb20711* mutant should be constructed to characterize the role of the *SMb20711* gene in D-*chiro*-inositol catabolism.

Concerning the third question: The *iolA* gene in *Pseudomonas spp.* was found to be essential for valine degradation. In *S. meliloti,* the *iolA* gene was identified and it was shown that the *iolA* gene is indeed essential for *myo*-inositol catabolism as well as valine degradation (Kohler et al., 2011). To confirm that the mutated *iolA* gene is really the cause of the phenotype of the *iolA* mutant, the *iolA* mutant should be complemented. The hypothesis for this question is that when the wild type gene is provided in *trans*, the phenotype of the *iolA* mutant should be restored to the wild-type phenotype.

In summary, the work described in this thesis will shed further light on the intricacies of the inositol transport in the soil bacterium *Sinorhizobium meliloti.*

CHAPTER 2

MATERIAL AND METHODS

Bacterial strains and plasmids

S. meliloti and *E. coli* strains used in this study are shown in Table 1. Plasmids constructed and acquired are also shown in Table 1.

Table 1: Bacterial strains and plasmids used in this study

Sinorhizobium meliloti

WT 2011	Wild type strain, Sm^R derivative of SU47	Meade et al., 1977
IbpA	2011mTn5STM.2.01.E03 *ibpA::gus*, Sm^R, Km^R	Pobigaylo et al., 2006
WIOLA	2011mTn5STM.4.03.B06 *iolA::gus*, Sm^R, Km^R	Pobigaylo et al., 2006
IbpB	2011 Δ*smb20072* Sm^R, Km^R, Sp^R	This study
IbpAIbpB	IbpA Δ*smb20072* Sm^R, Km^R, Sp^R	This study
IolI	2011 Δ*smb20711* Sm^R, Km^R	This study

Escherichia coli

DH5α	Strain used for transformations, *supE44 ΔlacU169* (Φ80 *lacZΔ* M15) *hsdR17 recA1 endA1 gyrA96 thi-1 relA1*	Sambrook et al., 1989
S17-1λpir	*pro thi hsdR*$^+$ Tc^R, Sm^R, chromosome::RP4-2 Tc::Mu-Kan::Tn7/λpir	Simon et al., 1983

Plasmids

pJQ200SK	Suicide vector, *sacB* gene, Gm^R, *mob*	Quandt and Hynes, 1993
pBluescript K/S+	Standard cloning vector, Ap^R, *lacZα*	Stratagene
pRK600	*mob, tra,* Cm^R	Finan et al., 1986
pTE3	broad host range expression vector, Tc^R	Egelhoff and Long, 1985
pBlueKan2	pBluescript with kanamycin cassette, Ap^R, Km^R	Dr. M. Goettfert, TU Dresden
pPH45Ω	Source for Ω fragment, Ap^R, Sm^R, Sp^R	Prentki et al., 1984
pIOLA	pTE3 containing 1.6 kb fragment of *iolA*	This study
pBS20072	1651 bp of the *SMb20072* gene cloned into pBluescript	This study
pBS20072Sp	2.2 kb EcoRI spectinomycin cassette from pPH45Ω cloned into pBS20072	This study
pJQ20072	3.6 kb PspOMI/SpeI fragment of pBS20072Sp cloned into pJQ200SK	This study
pBK20711L	766 bp XbaI/ BamHI left flanking region of the *SMb20711* gene cloned into pBlueKan2	This study
pBK20711LR	661 bp EcoRI/ PspOMI right flanking regions of the *SMb20711* gene cloned into pBK20711L	This study
pJQ20711	2.9 kb PspOMI/XbaI fragment of pBK20711LR containing Km cassette cloned into pJQ200SK	This study

Media and growth requirements

Full medium

Full medium for all *E. coli* strains was Luria-Bertani medium (LB) (Sambrook et al., 1989). This medium contained tryptone (10 g/L), yeast extract (5 g/L), and sodium chloride (5 g/L). Bacto-agar (15 g/L) was added for solid media.

Full medium for all *S. meliloti* strains was tryptone yeast medium (TY) (Beringer et al., 1974). This medium contained tryptone (5 g/L), yeast extract (3 g/L), and calcium chloride dihydrate (0.5 g/L). Bacto-agar (15 g/L) was added for solid media.

Minimal medium

Minimal M medium used for *S. meliloti* strains contained K_2HPO_4 (1.4 g/L), KH_2PO_4 (0.8 g/L), $CaCl_2$ x $2H_2O$ (0.02 g/L), $MgSO_4$ x $7H_2O$ (0.25 g/L), NaCl (0.2 g/L), $Fe(C_6H_5O_7)$ x H_2O (4 mg/L), Na_2MoO x $7H_2O$ (0.2 mg/L), $MnSO_4$ x $4H_2O$ (0.2 mg/L), H_2BO_2 (0.25 mg/L), $CoCl_2$ x $4H_2O$ (0.001 mg/L), thiamine HCl (1 mg/L), $CuSO_4$ x $5H_2O$ (0.02 mg/L), Ca-panthothenate (2 mg/L), $ZnSO_4$ x $7H_2O$ (0.16 mg/L), biotin (0.001 mg/L), EDTA (0.15 mg/mL), 0.1% NH_4Cl as the sole nitrogen source and either 0.2% *myo*-inositol, D-*chiro*-inositol or glycerol as the sole carbon source (Rossbach et al., 1994).

Growth conditions

All *E. coli* strains were incubated at 37°C. *E. coli* cultures were grown in 5 ml of LB broth in a rotary shaker (C25 Incubator Shaker, New Brunswick Scientific, Eddison, NJ) at 200 rpm overnight. *S. meliloti* strains were incubated at 28°C. *S.*

meliloti pre-cultures were grown in 5 ml of TY broth in a rotary shaker (C25 Incubator Shaker, New Brunswick Scientific, Eddison, NJ) at 200 rpm overnight.

Antibiotics

Antibiotics used in this study were purchased in powdered form. They were dissolved in de-ionized water (or 100% ethanol for chloramphenicol). Stock solutions were filter sterilized and stored in sterile 15 ml conical tubes. Stock solutions were stored in -20° C for long-term storage. Stock solution and culture concentrations are listed in Table 2 below.

Table 2: Antibiotics used in these studies

Antibiotic and Solvent	**Concentration of Stock (mg/ml)**	**Concentration used for *S. meliloti* (µg/ml)**	**Concentration used for *E. coli* (µg/ml)**
Ampicillin	100	-	100
Cloramphenicol	30	-	30
Gentamycin	30	100	15
Kanamycin	100	200	25
Spectinomycin	100	100	20
Streptomycin	100	250	25
Tetracycline	1	10	10

Growth studies

S. meliloti pre-cultures were grown in 5 ml TY broth with the appropriate antibiotics for 48 hours. Pre-cultures were inoculated into minimal media containing 0.2% of the carbon source of interest in a ratio of 1:100. Cultures were grown in a shaking incubator and the growth was measured using a spectrophotometer (DU-640 spectrophotometer, Beckman Coulter, Brea, CA) at 600 nm wavelength (OD_{600}) every 24 hours for 10 days continuously. Each growth study was carried out in triplicates, and values represent the average of three-independent experiments ± SEM.

Agarose gel electrophoresis

Agarose gels for DNA evaluations were prepared using 0.7% agarose dissolved in sodium borate (SB) buffer (10 mM NaOH; H_3BO_3 added to reach pH 8.5). The concentration of agarose was varied inversely to the size of the DNA fragment to be visualized. Electrophoresis was performed in SB buffer at 80 volts for up to an hour depending on the size of the DNA fragments.

10% of loading dye was added to the DNA sample before loading the sample into the agarose gel. Loading dye consisted of 0.25% xylene-cyanol FF, 0.25% bromophenol blue and 0.15% glycerol. The mixture was then loaded into the wells. The 1 kb DNA extension ladder from Invitrogen Life Technologies (Carlsbad, CA) was added onto each gel as the DNA size standard.

After electrophoresis, agarose gels were placed in 0.06 µl/ml ethidium bromide in SB buffer for staining. The amount of time needed for staining varied

from 10 to 20 minutes depending on the age of the ethidium bromide bath. After staining, gels were transferred in a glassware dish containing dH_2O to the KODAK Gel Logic 1500 Imaging System (Rochester, NY). Ultraviolet transillumination was used to visualize the DNA in the agarose gel. Camera exposures varied from 1 to 3 seconds depending on the intensity of the DNA bands. Pictures were saved as jpg images.

Polymerase Chain Reaction (PCR)

PCR was carried out in volumes of 25 µl or 50 µl. As template, one bacterial colony was resuspended in 5 µl of dH_2O. 2 µl of template was added into the reaction tube. Primers were added to a final concentration of 10 µM. Reaction buffers and dNTPs were added to the final concentrations recommended by the supplier, and the final volumes of the reaction were adjusted with dH_2O. In general, amplifications of less than 3 kilobases (kb) were performed with FlashTaq 2X MeanGreen Master Mix (Syzygy Biotech, Grand Rapids, MI). Amplifications of larger segments of DNA that was greater than 3 kb were performed with LongAmp Taq DNA Polymerase (NEB, Ipswich, MA).

PCR product purification using gel purification

Fragments of the desired size were excised from the electrophoresed and ethidium bromide stained agarose gel with a clean scalpel. Excised fragments were purified using Wizard Plus SV Gel and PCR Clean-Up system (Promega, Fitchburg, WI) following the protocol provided by the manufacturer. Gel fragments that were excised from the agarose gel were cleaned using Zymoclean™ Gel DNA Recovery Kit

(Zymo Research, Irvine, CA) following the protocol provided by the manufacturer. The DNA obtained was stored in a -20 °C freezer.

Restriction digests

Restriction digests were carried out in a total volume of 20 µl using the appropriate restriction endonuclease. Amount of DNA needed for restriction digests varied depending on the DNA concentration estimated from the agarose gel visualization. Endonucleases and buffers were acquired from New England Biolabs (Ipwich, MA). DNA restriction digests were carried out according to the manufacturer's protocol.

Ligations

Ligations were carried out in a total volume of 20 µl using 1 µl of T4 DNA ligase and 2 µl of T4 ligase buffer acquired from New England Biolabs (Ipwich, MA). Ligations were incubated overnight at 16 °C water bath according to the manufacturer's protocol.

Chemically competent cells

E. coli strain DH5α was used to generate competent cells needed for transformation purposes. A pre-culture of *E. coli* DH5α was used to inoculate sterile LB broth in the ratio of 1:100. The culture was incubated in a 37 °C shaker for 1 hour and 30 minutes, until the cells reached an OD_{600} ≈0.2. The bacterial suspension was then centrifuged (Sorvall RC-5B PLUS Centrifuge, Newtown, Canada) at 5,000 rpm (4,300 x g) for 10 minutes at 4 °C. The supernatant was removed and the pellet was resuspended in 20 ml of 100 mM ice-cold $CaCl_2$. The bacterial suspension was

left on ice for at least 30 minutes followed by centrifugation at 5,000 rpm (4300 x g) for 10 minutes at 4 °C. The supernatant was discarded once again and the pellet was resuspended in 2 ml of 100 mM ice-cold $CaCl_2$. Five hundred µl of the bacterial suspension were transferred to 4 sterile 1.5 ml Eppendorf tubes for storage. Cells were stored at 4°C and used for up to 48 hours. Un-used cells were stored in -80 °C with 20% glycerol for future use.

Isolation of plasmid DNA

The volume of cultures used for isolating plasmid DNA depended on the plasmid copy number. Either 1.4 ml (high copy number) or 5 ml (low copy number) of *E. coli* cultures containing the appropriate antibiotics were pelleted by centrifugation (Eppendorf Centrifuge 5415D, Brinkman Instruments, Westbury, NY) at 5,000 rpm (2,500 x g) for 10 minutes. Plasmids were isolated and purified using the Zyppy ™ Plasmid Miniprep Kit (Zymo Research, Irvine, CA) following the manufacturer's protocol. DNA was eluted in 20 µl of zippy elution buffer and stored in a -20 °C freezer for future use.

Transformation

One hundred µl of chemically competent *E. coli* cell were mixed with 10 µl of ligation mixture and 90 µl of dH_2O in a 1.5 ml micro-centrifuge tube. The mixture was chilled on ice for the first 30 minutes, followed by a heat shock at 42 °C for 1 minute. After heat shock, the mixture was returned to the ice bath for five minutes. One ml of Super Optimal Broth (S.O.C) was added to each mixture. The mixtures were then transferred and taped down laterally to a 37 °C rotary shaker (C25

Incubator Shaker, New Brunswick Scientific, Edison, NJ) at 200 rpm for approximately 90 minutes. Lastly, 150 µl of each mixture were plated onto LB agar plate with the appropriate antibiotics and incubated overnight in the 37 °C incubator.

Primers

Table 3: Primers used in these studies

iolA forward	ATTAATGCATCGATCATGAGGGCACAATCAAGGG
iolA reverse	ATTAGGATCCGAAGGAGGCTCCGATTGG
SMb20072 forward	ATTAGGGCCCGATCTGGACG
SMb20072 reverse	CACCTCACTAGTCGCAATGCCTGTGAATG
ELC1 (*SMb20711* left forward)	ATTATCTAGAGACCGGCTCCGGTCACACGAT
ELC2 (*SMB20711* left reverse)	ATTAGGATCCGCAAGGGCTTTCACCTCCTC
ELC3 (*SMb20711* right forward)	ATTAGAATTCTCATTCGAGCCCTTTGCCCCTTCC
ELC4 (*SMb20711* right reverse)	ATTAGGGCCCTTGACATAGACCAGCGGAAT

Underlined bases showed restriction sites that were added to the primers to facilitate cloning of the resulting PCR products.

Di-parental mating

A pre-culture of the *E. coli* S17-1 strain containing the transferrable plasmid pJQ20711 was grown in the 37°C rotary shaker for 24 hours in LB broth with appropriate antibiotics. A pre-culture of *S. meliloti* wild type 2011 was grown in the 28°C rotary shaker for 48 hours in TY broth with appropriate antibiotics. One ml of the *S. meliloti* wild type 2011 and 200 µl of *E. coli* S17-1 were mixed, and then centrifuged at 9,000 rpm (7,500 x g) for 90 seconds using a tabletop centrifuge. Supernatants obtained during the process were discarded and the pellets were washed in 1 ml LB broth to remove any antibiotic residues. The mixtures were centrifuged at 9,000 rpm (7,500 x g) for 90 seconds; supernatants were discarded. Pellets obtained were re-suspended in 150 µl of TY broth. All re-suspensions along with controls were spotted onto TY agar plates and incubated overnight in a 28°C standing incubator.

The following day, all plates were removed from the incubator and flooded with 4 ml of 10 mM $MgSO_4$. The cells were then scraped up using a sterile spatula, and transferred to 15 ml conical tubes. The conical tubes were vortexed briefly before dilution. The mixtures containing *S. meliloti* and *E. coli* S17-1 with transferable plasmids were serially diluted (10^{-2}, 10^{-4}, 10^{-6}, and 10^{-8}), except the controls. Of each mixture, 150 µl were plated onto TY agar plates with the appropriate antibiotics.

Tri-parental mating

Conjugation of plasmids from *E. coli* to *S. meliloti* was accomplished using a triparental mating protocol from Dr. Sharon Long, Stanford University, California with slight modifications (http://cmgm.standford.edu/biology/long/protocols.html). Pre-cultures of an *E. coli* helper strain that contained the pRK600 plasmid and *E. coli* DH5α containing the transferable plasmids were grown in a 37°C rotary shaker for 24 hours in LB broth with appropriate antibiotics. A pre-culture of *S. meliloti* wild type 2011 was grown in a 28°C rotary shaker for 48 hours in TY broth with appropriate antibiotics. One and a half ml of both *E. coli* helper and donor strain along with one and a half ml of *S. meliloti* strain were centrifuged each at 5,000 rpm (2,320 x g) for 10 minutes using a tabletop centrifuge (Eppendorf Centrifuge 5415D, Brinkman Instruments, Westbury, NY). Supernatants obtained during the process were discarded and the pellets were washed in 800 µl LB broth to remove any antibiotic residues. The mixtures were centrifuged at 5,000 rpm (2,320 x g) for 10 minutes; supernatants were discarded. Pellets obtained were re-suspended in 150 µl LB broth. Then, 50 µl of the *S. meliloti* strain were mixed with 15 µl of *E. coli* helper and donor strain and spotted onto LB agar plate. All the other pair-wise controls were spotted onto TY agar plates and incubated at 28°C in a standing incubator overnight and treated as described in the di-parental mating procedure.

Complementation

The wild-type genes that were required for complementation were PCR-amplified using the appropriate primers that contained a NsiI site in the *iolA* forward primer and a BamHI site in the *iolA* reverse primer (Table 3). These particular enzymes were used in order to accomplish directional cloning of the wild-type *iolA* gene into the broad host range expression vector, pTE3. The wild-type gene was ligated into the pTE3 vector, which contains the *Salmonella trp* promoter that will constitutively express in *S. meliloti* (Egelhoff et al., 1985). Ligation mixtures were transformed using chemically competent *E. coli* cells, and selected on LB agar plates that contained tetracycline. The resulting construct was then conjugated into the mutant to be complemented via tri-parental mating.

β-Glucuronidase assays

S. meliloti pre-cultures were inoculated in a ratio of 1:100 into 10 ml of minimal media containing 0.2% glycerol as the sole carbon source and 0.1% NH_4Cl as the nitrogen source. After 24 hours in a 28°C rotary shaker, the culture usually reached an optical density (OD_{600}) between 0.7 to 1.0 indicating that the cultures were in an exponential growth phase. The culture was divided into six 1.5 ml eppendorf tubes and centrifuged (Eppendorf Centrifuge 5415D, Brinkman Instruments, Westbury, NY, USA) at 7,000 rpm (4,500 x g) for 10 minutes. The pellets obtained were then resuspended in 3 ml of minimal media with 0.2% of glycerol or 0.1% *myo*-inositol and 0.1% glycerol as the sole carbon source. Cultures were returned to the 28°C rotary shaker for 2 and 4 hours. Aliquots of 0.5 ml of the suspensions were removed from the cultures and the OD_{600} was recorded. Two aliquots of 350 µl were taken from the control culture with glycerol only and the test cultures with glycerol and *myo*-inositol as the carbon source. Each 350 µl aliquot was centrifuged at 7,000 rpm (4,500 x g) for 10 minutes. The pellets obtained were resuspended in general extraction buffer (GEB Buffer: 50 mM sodium phosphate buffer pH 7, 0.6% β-mercaptoethanol, 10 mM EDTA, 1% Triton X100 and 0.1% sodium lauryl sarcosine) and incubated at 37°C for 15 minutes. After 15 minutes of pre-incubation, 35 µl of 20 mM 4-nitrophenyl-β-D-glucuronide (PNPG) were added as substrate to each suspension and further incubated at 37°C. For the wild type strain, 100 µl of the suspension were removed after 5, 10 and 15 minutes and 800 µl of the stop solution (400 mM Na_2CO_3) were added. For the mutant strains, 100 µl of suspension were removed after 1, 2, and 3 minutes and 800 µl of

the stop solution were added. Before taking the optical density measurements, the cell debris was removed by centrifugation at 13,200 rpm for one minute. The intensity of the yellow color formed was measured spectrophotometrically at 405 nm (OD_{405}). The reaction rate was calculated as nmol of *p*-nitrophenol produced per min per OD_{600}.

Equation: Reaction rate = Slope/ (0.02 x original volume x OD_{600})

Where: Slope = average slope of the OD_{405} plotted vs time in minutes

0.02 = based on the molar extinction coefficient for *p*-nitrophenol

V = the volume of cells used in the reaction (0.1ml)

OD_{600} = optical density of the cell suspension

NAD(H)-dependent dehydrogenase assays

S. meliloti pre-cultures were inoculated 1:100 into a 500 ml Erlenmeyer flask containing 100 ml minimal media with 0.1% NH_4Cl as nitrogen source, 0.2% glycerol as carbon source and lastly 0.02% *myo*-inositol as inducer. Late exponential phase cultures with OD_{600} ≈1 to 1.25 were harvested by centrifugation at 7,000 rpm (6,000 x g). Pellets collected were washed with 40 mM HEPES buffer (pH 7). Cell extracts were prepared with a sonicator at 50 W with 24 x 30 seconds sonication periods (Misonix XL-2020, Farmingdale, NY). *myo*-Inositol dehydrogenase activities were determined at room temperature (21–25 °C). Each 1 ml reaction mix contained 50 mM NH_4Cl, 50 mM Na_2CO_3, 100 µl cell extract and 0.4 mM NAD^+. A baseline background reduction of NAD^+ in the absence of substrate was established at a wavelength of 340 nm. The increase in absorbance (A_{340}) in the presence of 25 mM *myo*-inositol was monitored for 3 minutes. Protein content of the cell extracts was determined using the Bradford assay (Pierce Coomassie Plus The Better Bradford™ Assay Kit, Thermo Fisher Scientific, Rockford, IL). The specific *myo*-inositol dehydrogenase activity was expressed as nmol NAD^+ reduced min^{-1} mg $protein^{-1}$ ± SEM. The values represent the mean of two independent experiments; each of the experiment was performed in duplicate.

Bioinformatics analysis

S. meliloti DNA and protein sequences were retrieved from the *S. meliloti* 1021 genome annotation website (https://iant.toulouse.inra.fr/bacteria/annotation/cgi/rhime.cgi). Identity and similarity searches were carried out using the NCBI Blast program (http://blast.ncbi.nlm.nih.gov/Blast.cgi) and amino acid sequence alignments were performed with the ClustalX program (http://www.clustal.org/clustal2). Metabolic pathways were identified with the KEGG database (http://www.genome.jp/kegg).

Plant inoculation assays

Medicago sativa (alfalfa) seeds were surface sterilized using 70% ethanol for 3 minutes, followed by 3 minutes with 0.1% mercury chloride ($HgCl_2$). Seeds were then rinsed three times with sterile dH_2O.

In preparation for seed germination, folded Whatman 3MM filter paper (4 cm x 8 cm) was inserted into 20 x 25 mm glass tubes. Twenty ml of B&D medium(Broughton & Dilworth, 1971) containing KH_2PO_4 (136.1g/l), K_2HPO_4 (228.28 g/l), K_2SO_4 (84 g/l), $CaCl_2$ x H_2O (294.1 g/l), Fe ($C_6H_5O_7$) x H_2O (6.7 g/l), $MgSO_4$ x $7H_2O$ (123.3 g/l), $MnSO_4$ (338 mg/l), $ZnSO_4$ x $7H_2O$ (288 mg/l), $CuSO_4$ x $5H_2O$ (100 mg/l), $CoSO_4$ x $7H_2O$ (56 mg/l), Na_2MO_4 x $2H_2O$ (48 mg/l), H_3BO_3 (247 mg/l) was added into each glass tube followed by sterilization. The surface sterilized seeds were put onto the Whatman 3MM filter paper to allow germination for one week. The seeds were grown in room temperature under 16 hours of fluorescent light and 8 hours of darkness for the whole duration of the experiment.

Bacterial cultures for inoculation were prepared in 50 ml of TY broth. The wild type *S. meliloti* and mutants were harvested by centrifugation at 7,000 rpm (4,000 x g) for 10 minutes (Sorvall RC-5B PLUS Centrifuge, Newtown, Canada). Each pellet was washed once with 50 ml of sterile dH_2O, centrifuged at 7,000 rpm (4,000 x g) for 10 minutes and resuspended in 50 ml sterile dH_2O. Cell density was measured spectrophotometrically at 600 nm.

The germinated plants were inoculated with either wild-type *S. meliloti* or the mutants strains. Ten plants were inoculated per strain. For inoculation, one ml of each *S. meliloti* wild-type or mutant strain was added into the glass tubes containing the germinated plants. Nodule formation was observed visually after 8 weeks of growing the plants in a plant growth chamber.

CHAPTER 3

RESULTS

Role of the *SMb20072* gene encoding a periplasmic binding protein

It was previously shown that *S. meliloti* 2011 is able to use *myo*-, D-*chiro*-, and *scyllo*-inositol as sole carbon sources (Kohler et al., 2010). The *ibpA* gene is predicted to encode a periplasmic binding protein (Fig. 6) working together with an ABC transporter that is involved in *myo*-inositol transport (http://iant.toulouse.inra.fr).

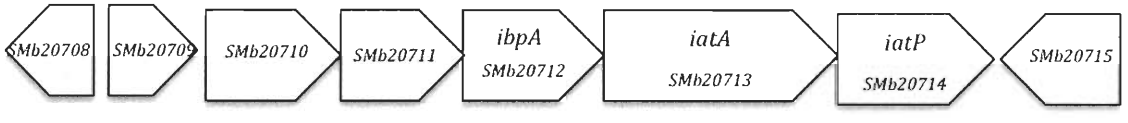

Figure 6: Genetic map of a *S. meliloti* genomic region functioning in inositol transport and catabolism. The map represents of the nucleotide sequence from 1,510,373 to 1,519,401 of the *S. meliloti* genome. The open arrows denote the open reading frames.

Previously, studies were done to test whether this transporter was involved in the transport of inositols (Boutte et al., 2008; Thwaites, 2013). Boutte et al (2008) showed that the *ibpA* mutant was not capable of utilizing *myo*-inositol as the sole carbon source. However, Thwaites (2013) showed that the *ibpA* mutant exhibited a delayed growth with *myo*-inositol as the sole carbon source. In order to reconfirm that this specific periplasmic binding protein is in fact used for transporting inositol compounds, an *ibpA* mutant that contained a mini-Tn*5* insertion (Pobigaylo et al., 2006) was used to perform growth studies. Growth studies were performed using *S.*

meliloti wild-type strain and the *ibpA* mutant that were grown in minimal media with either glycerol or *myo*-inositol as the sole carbon source (Fig. 7).

The wild type *S. meliloti* 2011 strain reached an $OD_{600} \approx 2.7$ either with glycerol or *myo*-inositol after 10 days, signifying a normal growth (Fig. 7A). The *ibpA* mutant reached an $OD_{600} \approx 2.7$ only with glycerol, but stayed below $OD_{600} \approx 1.5$ with *myo*-inositol as the sole carbon source. The *ibpA* mutant could regain growth after three days (Fig. 7B). This suggests that the *ibpA* gene product is indeed involved in the initial transport of *myo*-inositol, but over time these inositols may enter the cells via an alternative pathway.

A.

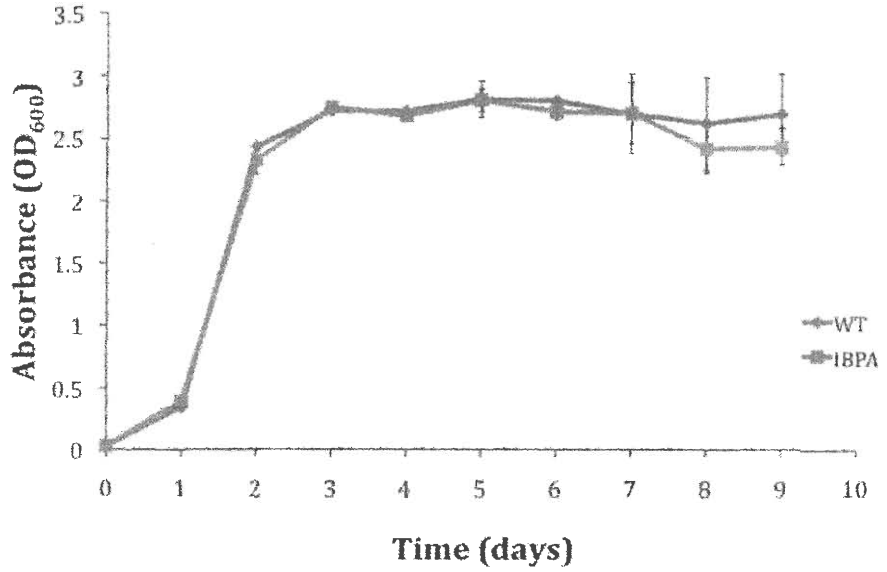

B.

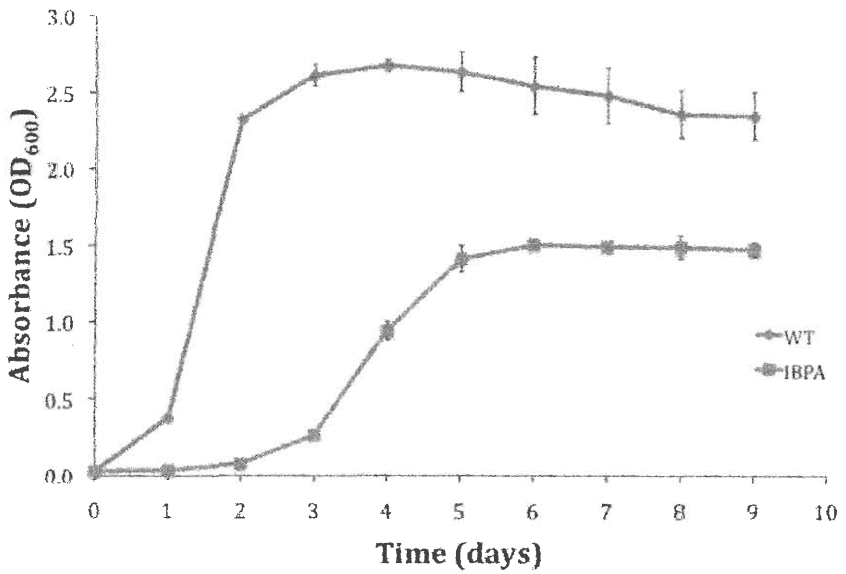

Figure 7: Growth of *S. meliloti* WT 2011 and *ibpA* mutants in minimal media containing either 0.2% of glycerol (A) or 0.2% *myo*-inositol (B) as the sole carbon source. Growth was measured spectrophotometrically at 600 nm for 10 days. This experiment was performed in triplicate. Error bars denote the standard error of the mean (SEM).

The *S. meliloti* genome revealed the presence of a gene encoding another periplasmic-binding protein, *SMb20072*, which is induced by *myo*-inositol besides the *ibpA* gene (Mauchline et al., 2006). In order to characterize the role of the second periplasmic-binding protein that is induced by *myo*-inositol, we decided to construct a single mutant with an insertion in the *SMb20072* gene (Fig. 8), which we later called *ibpB* and a double mutant with insertions in both the *ibpB* and the *ibpA* genes.

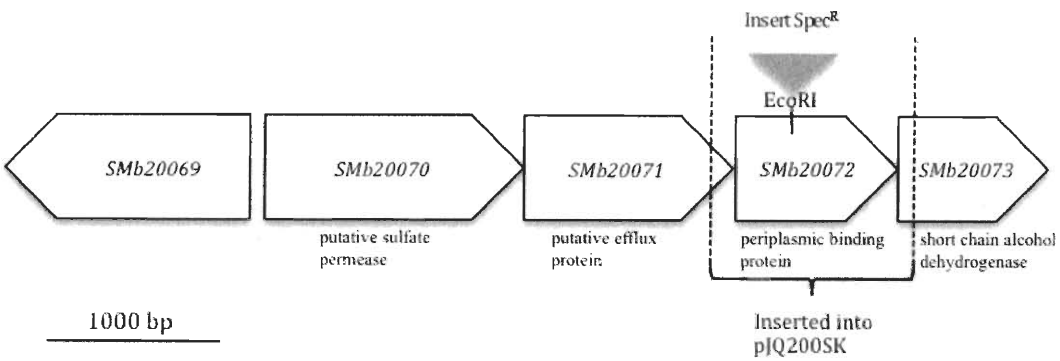

Figure 8: Genetic map of a second *S. meliloti* genomic region functioning in inositol transport. The map shows the nucleotide sequence from 76,205 to 83,626 of the *S. meliloti* genome. The open arrows denote the open reading frames. The grey triangle indicates the insertion of the spectinomycin cassette (Spec^R). The dotted line indicates the region that was inserted into the pJQ200SK plasmid.

To construct the *ibpB* single mutant and the *ibpAibpB* double mutant, a fragment of 1651 bp was obtained by PCR amplification using the *SMb20072* forward and *SMb20072* reverse primers that contained the PspOMI and SpeI restriction sites, respectively (Table 3). The PCR product was cloned into the pBluescript SK^+ vector. This resulting plasmid, pBS20072, was digested with EcoRI resulting in a single cut in the *SMb20072* gene. A 2.2 kb spectinomycin cassette from pPH45Ω was inserted into the *SMb20072* gene resulting in the pBS20072Sp plasmid. The pBS20072Sp plasmid was digested with PspOMI/SpeI in order to remove the gene of interest along with the spectinomycin cassette insertion that is 3.8 kb in size. This fragment was inserted into a suicide vector pJQ200SK resulting in plasmid pJQ20072. The mutated gene replaced the wild-type gene as described in Material and Methods. The mutants were confirmed by PCR using the *SMb20072* forward and reverse primers (Table 3). The length of the *SMb20072*::Spec fragment is 3851 bp (Fig. 9).

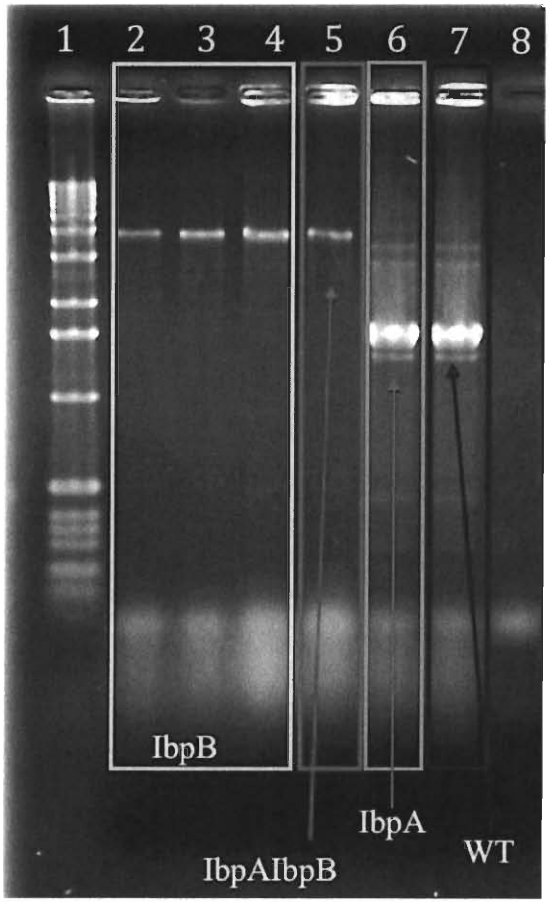

Figure 9: Confirmation of the single *ibpB* mutant and the *ibpAibpB* double mutant by PCR. Photograph of an agarose gel after electrophoresis and ethidium bromide staining. SMb20072 forward and SMb20072 reverse were used as primers (Table 3).

Lane 1: 1kb extension ladder from NEB.

Lane 2, 3, and 4: The *SMb20072*::Sp PCR product (3851 bp) with the *S. meliloti ibpB* single mutants as template.

Lane 5: The *SMb20072*::Sp PCR product (3851 bp) with the *S. meliloti ibpAibpB* double mutant as template.

Lane 6: The PCR product of the *SMb20072* gene (1651 bp) with the *S. meliloti* 2011 *ibpA* mutant as template.

Lane 7: The PCR product of the *SMb20072* gene (1651 bp) with the *S. meliloti* 2011 wild type as template.

The *S. meliloti* 2011 wild type and the *ibpA, ibpB* and *ibpAibpB* double mutants were used to perform the following growth studies (Fig. 10). All strains were grown in minimal media with either 0.2% of *myo*-inositol, D-*chiro*-inositol, pinitol or glycerol (control) as the sole carbon source. The turbidity of the cultures was measured every 24 hours for 10 days continuously. The *S. meliloti* wild type 2011 strain reached an OD_{600} ≈2.9 with all carbon sources, signifying normal growth (Fig. 10 A, B, C, D). The *S. meliloti* single and double mutants were able to reach optical densities comparable to the wild type in minimal media when glycerol was offered as the sole carbon source; they all reached an OD_{600} ≈2.5 with the control carbon source (Fig. 10A).

The *S. meliloti ibpA* single mutant showed a delayed growth when *myo*-inositol or D-*chiro*-inositol was offered as the sole carbon source. The *ibpA* mutant regained growth after three days, which is consistent with the results obtained previously by Thwaites (2013). In contrast, the *S. meliloti ibpB* single mutant did not show delayed growth with *myo*-inositol or D-*chiro*-inositol as the sole carbon source, but nevertheless the growth was not comparable to the wild-type strain. The *ibpB* single mutant reached an OD_{600} ≈2.2 with *myo*-inositol or D-*chiro*-inositol as the sole carbon source. However, the *ibpAibpB* double mutant only reached an OD_{600} ≈0.2 with *myo*-inositol (Fig. 10B) or D-*chiro*-inositol (Fig. 10C) even after ten days of incubation. These results confirm that the observed growth delay of the *ibpA* mutant with *myo*-inositol or D-*chiro*-inositol is due to the presence of a second inositol transporter that is encoded by the *ibpB* gene.

In addition, it was previously shown that *S. meliloti* 2011 is able to use pinitol as the sole carbon source (Thwaites, 2013). Growth studies were performed with *S. meliloti* wild-type strain and the mutants in minimal media with pinitol as the sole carbon source. The wild type reached an OD_{600} ≈2.5 whereas the *ibpA* mutant reached OD_{600} ≈0.3 with pinitol as the sole carbon source for the first three days. After three days, the *ibpA* mutant regained growth and reached an OD_{600} ≈1.5. The *ibpB* mutant reached an OD_{600} ≈1.8 when pinitol was provided as the sole carbon source. However, the *ibpAibpB* double mutant only reached an OD_{600} ≈0.1 throughout the length of the experiment (Fig. 10D).

This confirmed that both the *ibpA* and *ibpB* genes are needed for transporting inositols, including the *myo-* and D-*chiro*-inositol isomers, as well as pinitol.

A.

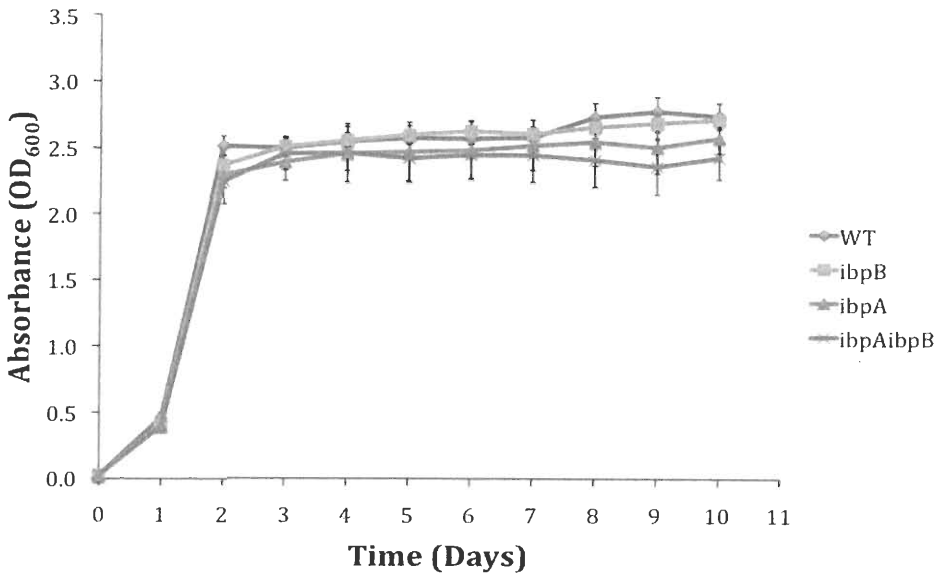
Absorbance (OD_{600})
3.5
3.0
2.5
2.0
1.5
1.0
0.5
0.0
0
1
2
3
4
5
6
7
8
9
10
11
Time (Days)
WT
ibpB
ibpA
ibpAibpB

B.

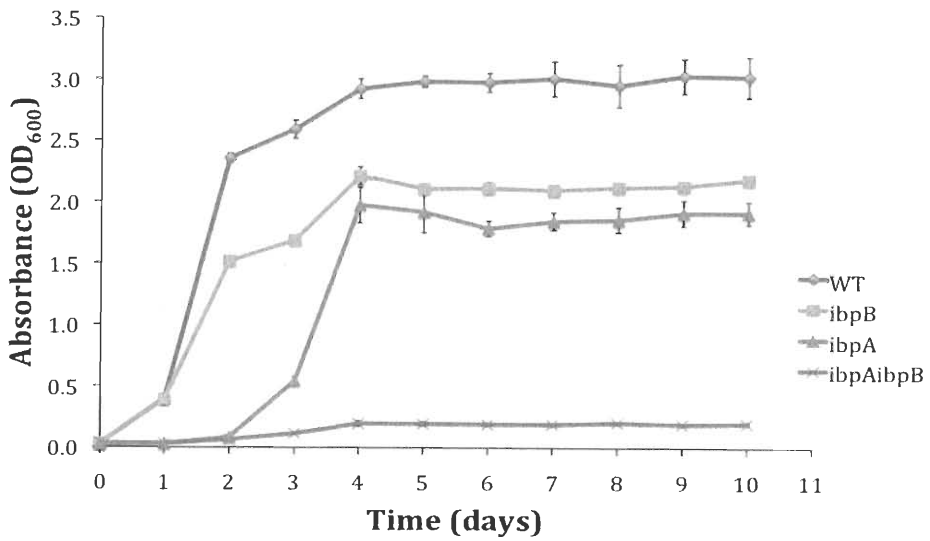
Absorbance (OD_{600})
3.5
3.0
2.5
2.0
1.5
1.0
0.5
0.0
0
1
2
3
4
5
6
7
8
9
10
11
Time (days)
WT
ibpB
ibpA
ibpAibpB

C.

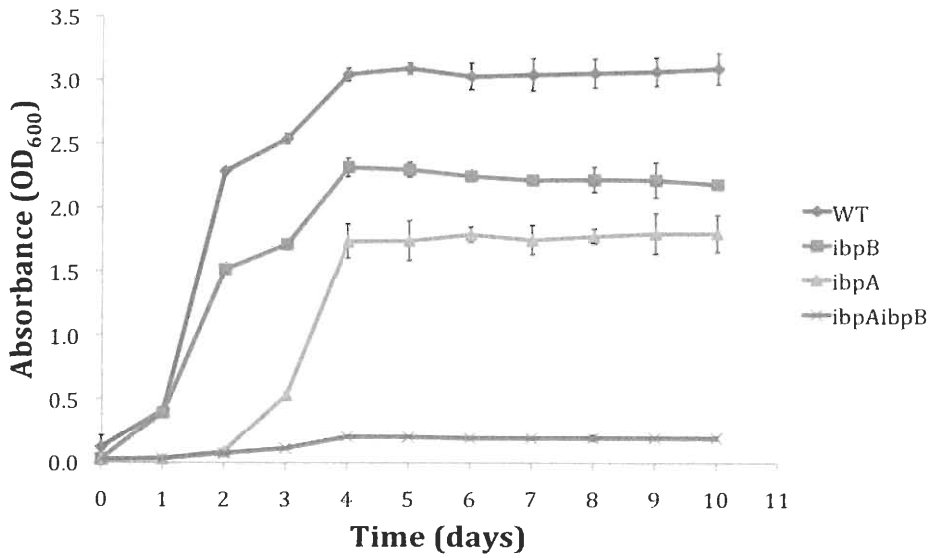

D.

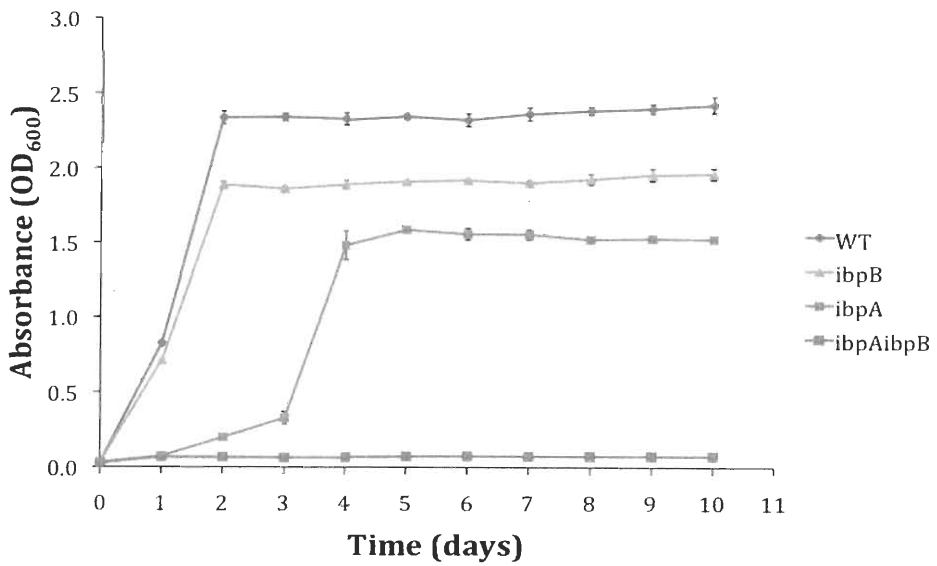

Figure 10: Growth of *S. meliloti* WT 2011 and mutants in minimal media containing either 0.2% glycerol (A), 0.2% *myo*-inositol (B), 0.2% D-*chiro*-inositol (C) or 0.2% pinitol (D) as the sole carbon source. Growth was measured spectrophotometrically at 600 nm for 10 days. This experiment was performed in triplicate. Error bars denote the standard error of the mean (SEM).

The Clustal X program for multiple protein alignments revealed that the *S. meliloti* IbpA and the *C. crescentus* IbpA share 27% identical amino acids, whereas the *S. meliloti* IbpB and the *C. crescentus* IbpA share 26% identical amino acids. Nevertheless, the *S. meliloti* IbpA and IbpB share 59% identical amino acids (Fig 11). The crystal structure of the *C. crescentus* IbpA protein bound to *myo*-inositol has recently been determined (Herrou and Crosson, 2013). It was found that there are 11 residues in the ligand-binding cavity that make direct contact with the hydroxyl-group of *myo*-inositol. Of those, four residues appear to be in the same position in the *S. meliloti* IbpA and IbpB proteins: R178, N231, D258, Q278 (Fig. 11). Also, the bound *myo*-inositol is flanked by two phenylalanine residues (F51 and F52) that make van der Waals contact with IbpA in *C. crescentus* (Herrou and Crosson, 2013). Interestingly, the *S. meliloti* IbpA and IbpB only contain one phenylalanine residue (F51) at that position.

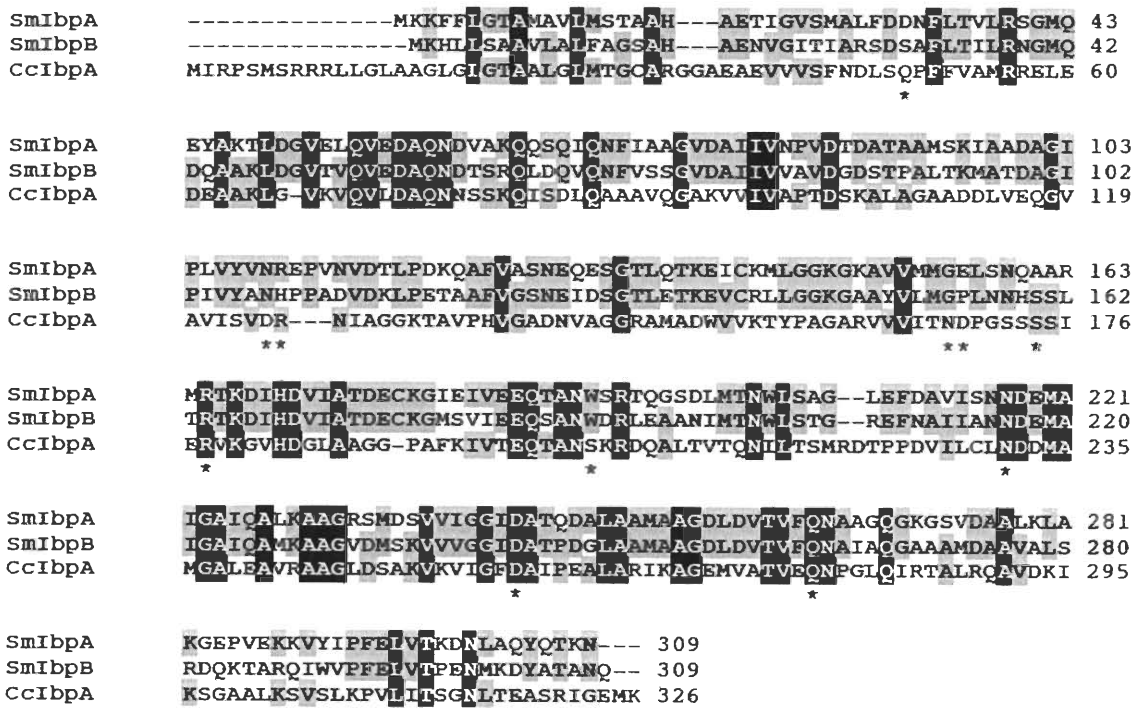

Figure 11: Amino acid sequence alignment of *S. meliloti* IbpA (SmIbpA), *S. meliloti* IbpB (SmIbpB) and *C. crescentus* IbpA (CcIbpA). Residues marked with asterisk were shown to be involved in interactions with *myo*-inositol (Herrou and Crosson, 2013). Black boxes highlight the residues that are identical in all proteins. Grey boxes highlight the residues that are identical in two of the three aligned proteins.

Role of the *SMb20711* gene encoding an inosose isomerase

According to the KEGG database (http://www.genome.jp), the SMb20711 gene that encodes a sugar epimerase has the same function as the *iolI* gene in *B. subtilis.* To construct a putative inosose isomerase mutant, a left flanking region of 766 bp and a right flanking region of 661 bp of the *SMb20711* gene were obtained by PCR amplification using the ELC1/ELC2 and ELC3/ELC4 primers that contained the XbaI/BamHI and EcoRI/PspOMI restriction sites, respectively (Table 3). The resulting PCR products were cloned into the pBlueKan2 vector to the left and to the right of the 1502 bp kanamycin cassette resulting in the pBK20711 plasmid (Fig. 12). The resulting pBK20711 plasmid was digested with PspOMI/XbaI in order to remove the gene of interest along with the kanamycin cassette. This 2929 bp long fragment was inserted into the suicide vector pJQ200SK resulting in plasmid pJQ20711. The mutated gene replaced the wild-type gene as described in Material and Methods. The mutant was confirmed by PCR using the ELC1/ELC4 primers (Table 3). The length of the *SMb20711::*Km was 2929 bp (Fig. 13).

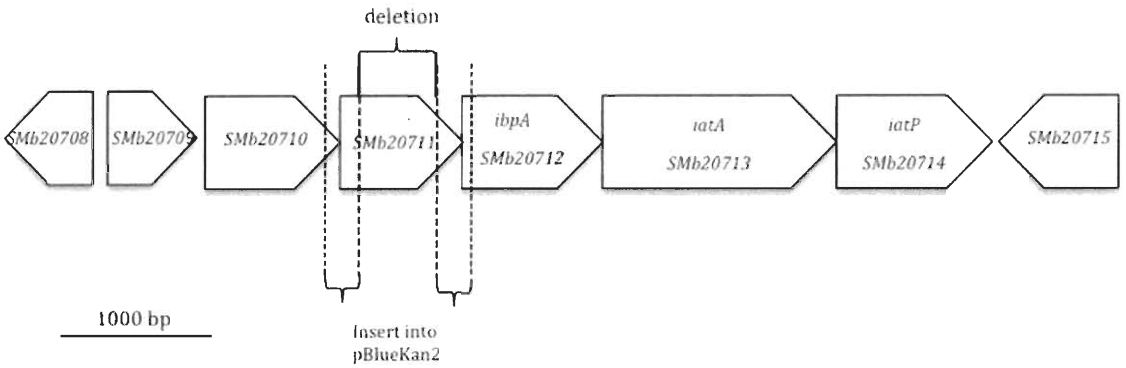

Figure 12: Genetic map of the *S. meliloti* genomic region functioning in inositol transport and catabolism. The map shows of the nucleotide sequence from 1,510,373 to 1,519,401 of the *S. meliloti* genome. The open arrows denote the open reading frames. The black bolded line indicates the region that was deleted before cloning. The dotted line indicates the region that was inserted to the left and to the right of the kanamycin cassette in the pBlueKan2 vector.

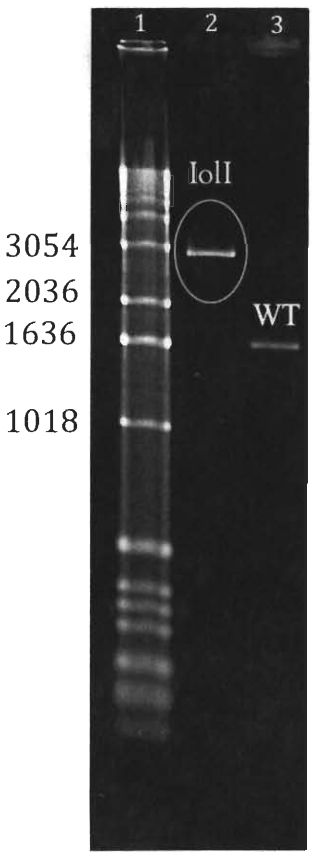

Figure 13: Confirmation of the IolI mutant by PCR. Photograph of an agarose gel after electrophoresis and ethidium bromide staining. Primers used were ECL1 and ECL4 (Table 3).

Lane 1: 1kb extension ladder from NEB.

Lane 2: The *SMb20711*::Km PCR product (2929 bp) with the *S. meliloti iolI* mutant as template.

Lane 3: The PCR product of the *SMb20711* gene (1613 bp) with the *S. meliloti* 2011 wild type as template.

The *S. meliloti* 2011 wild type and the *iolI* mutant were used to perform the following growth studies. Both strains were grown in D-*chiro*-inositol, *myo*-inositol or glycerol (control) as the sole carbon source. The *S. meliloti* wild type 2011 strain reached an OD_{600} ≈2.6 with all carbon sources, signifying the normal growth. The *iolI* mutant was able to reach optical densities comparable to the wild type in minimal media when glycerol was offered as the sole carbon source (Fig. 14A). However, the *iolI* mutant was unable to use D-*chiro*-inositol as the sole carbon source. The mutant did not grow even after ten days when D-*chiro*-inositol was offered as the sole carbon source (Fig. 14B). The *iolI* mutant reached a maximum of OD_{600} ≈0.3 even after ten days, which is 11% of the wild-type strain. Therefore, the product of the *SMb20711* gene seems to be essential for the growth with D-*chiro*-inositol as the sole carbon source.

The *S. meliloti iolI* mutant reached an OD_{600} ≈1.5 with *myo*-inositol as the sole carbon source, which is 40% less than the wild type (Fig. 14C). In addition, the *iolI* mutant reached an OD_{600} ≈1 with pinitol as the sole carbon source (Fig. 14D), which indicates that the growth for the *iolI* mutant was 60% less than the wild type. These data suggest that the *SMb20711* gene product might also be involved in *myo*-inositol and pinitol metabolism.

A.

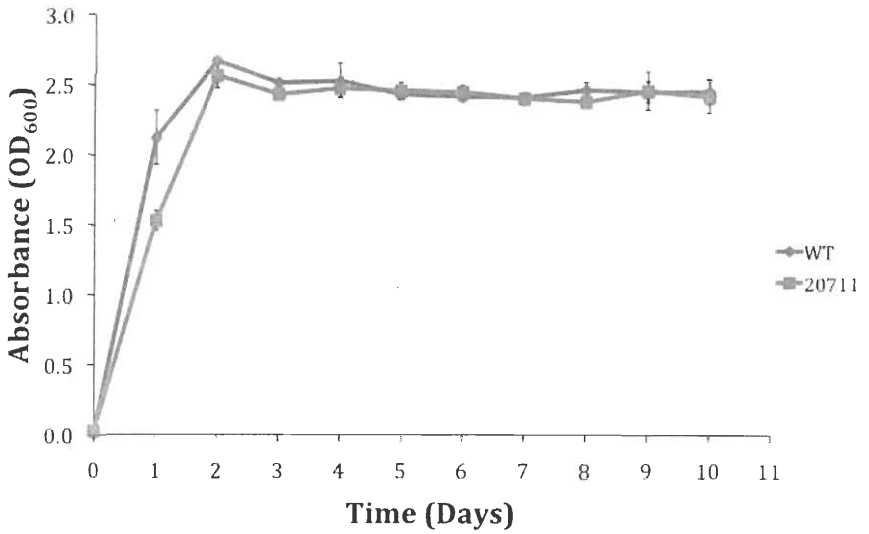
Absorbance (OD_{600})
3.0
2.5
2.0
1.5
1.0
0.5
0.0
0 1 2 3 4 5 6 7 8 9 10 11
Time (Days)
WT
20711

B.

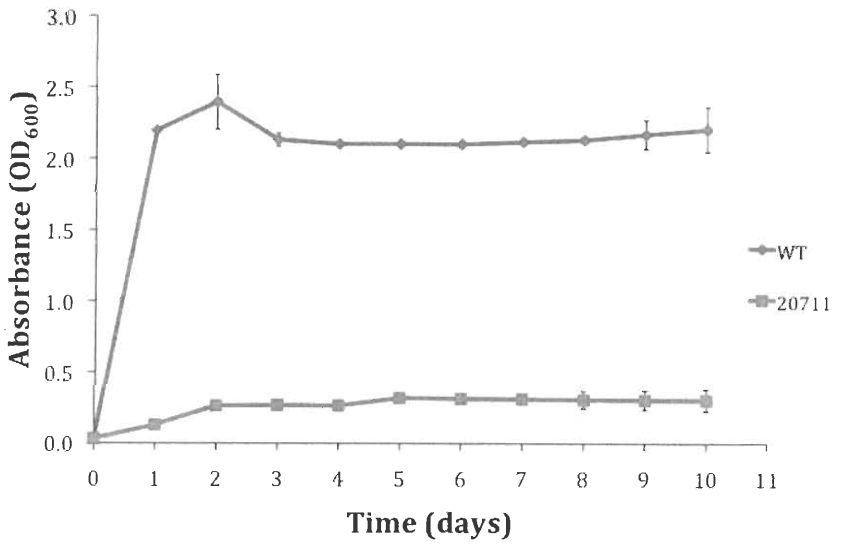
Absorbance (OD_{600})
3.0
2.5
2.0
1.5
1.0
0.5
0.0
0 1 2 3 4 5 6 7 8 9 10 11
Time (days)
WT
20711

C.

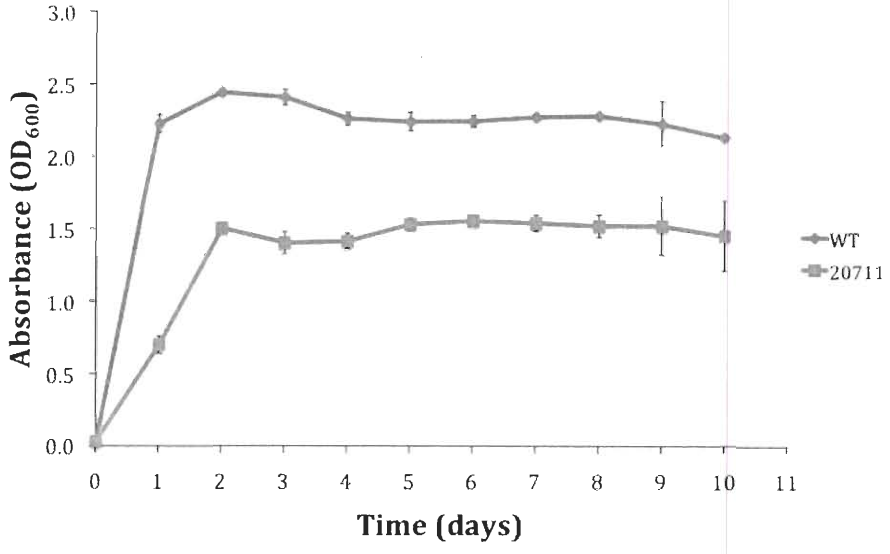

D.

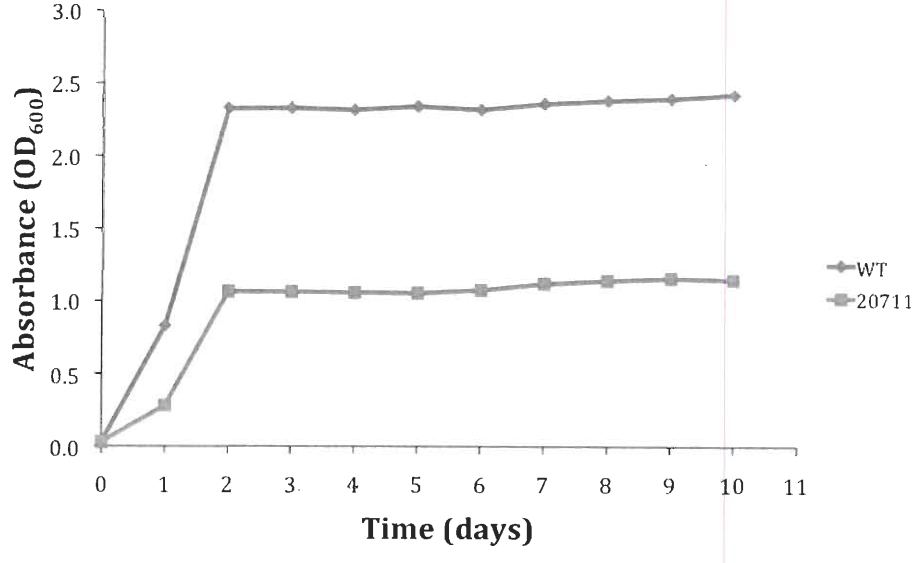

Figure 14: Growth of *S. meliloti* WT 2011 and mutants in minimal media containing either 0.2% glycerol (A), 0.2% D-*chiro*-inositol (B), 0.2% *myo*-inositol (C) or 0.2% pinitol (D) as the sole carbon source. Growth was measured spectrophotometrically at 600 nm for 10 days. This experiment was performed in triplicate. Error bars denote the standard error of the mean (SEM).

The Clustal X program for multiple protein alignments revealed that the IolI in *S. meliloti* and *S. fredii* share 81% identical amino acids, whereas the IolI of *S. meliloti* and *P. syringae* share 54% identical amino acids (Fig. 15). Interestingly, the IolI in *S. meliloti* and *B. subtilis* share only 21% identical amino acids. Based on these alignments, it is clear that the *iolI* gene product is more conserved among the closely related rhizobial and proteobacterial species (Fig. 15).

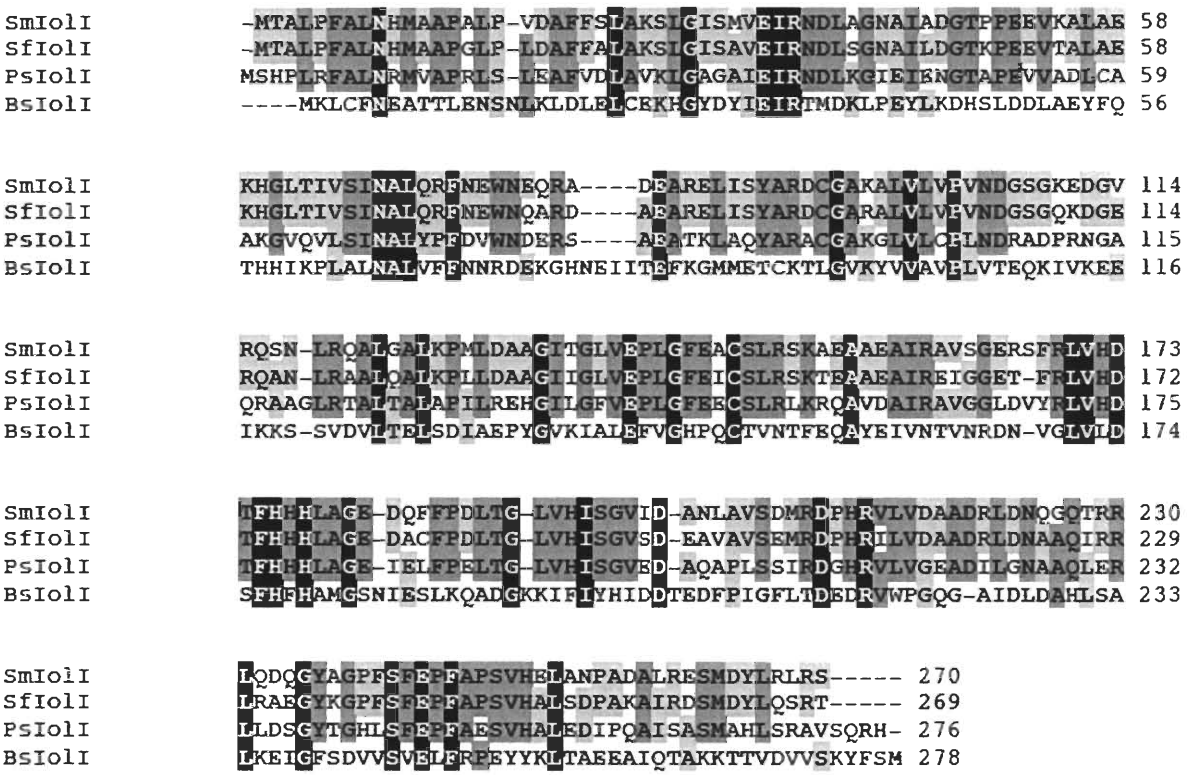

Figure 15: Amino acid sequence alignment of *S. meliloti* IolI (SmIolI), *S. fredii* IolI (SfIolI), *P. syringae* IolI (PsIolI) and *B. subtilis* IolI (BsIolI). Black boxes highlight the residues that are identical in all proteins. Dark grey boxes highlight the residues that are identical in three proteins. Light grey boxes highlight the residues that are identical in two proteins.

Predicted IolR-binding motifs upstream of the *ibpA, ibpB* and *iolI* genes

It was previously shown that the *S. meliloti iolR* gene product is involved in the regulation of the inositol catabolic genes (Kohler et al., 2011). IolR recognizes a conserved palindromic sequence (5'-GGAA$_{5-11}$TTCC-3') in the upstream region of the *iol* genes. The upstream regions of the *idhA, iolY, iolR,* and *iolC* genes each contain a putative IolR-binding motif (Table 4). Interestingly, the upstream region of the *ibpA, ibpB* and the *iolI* genes also contain a putative IolR-binding motif (5'-GGAA$_{5-11}$TTCC-3') with slight variations. These inositol transport and catabolism genes have yet to be investigated in *S. meliloti,* but our finding suggests that these genes are also IolR-regulated.

Table 4: The identified IolR-binding motifs of the *idhA, iolY, iolR, iolC* genes, as well as the predicted IolR-binding motifs of the *ibpA, ibpB* and *iolI* genes

Gene	IolR binding motif in the upstream region	Distance to start codon (bp)
idhA	5'-GGAATAAATATTCC -3'	42
iolY	5'-CGAACAAATATTCC -3'	72
iolR	5'-GGAACATCCGTTCT -3'	286
iolC	5'-AGAATGGAAATTCC -3'	100
iolI	5'-GGAACAAACGTTCC -3'	44
ibpB	5'-AGAACTTGTATTCC -3'	44
ibpA	5'-GGAAGAAGATCGCGTTCC -3'	44

Nodulation assay

In order to see if the ability to utilize inositols may play a role in plant-bacteria interactions, the ability of the *ibpA, ibpB,* and the *iolI* mutants to nodulate alfalfa was tested. The wild type and the individual mutant strains were inoculated onto alfalfa plants. Our results showed that the *ibpA, ibpB* and the *iolI* mutants of *S. meliloti* nodulated alfalfa successfully when inoculated onto plant individually (data not shown).

Further characterization of the *iolA* gene encoding a methyl malonate semialdehyde dehydrogenase

Before I started my thesis work, I had shown that the *iolA* gene is not only essential for *myo*-inositol catabolism, but also important for valine degradation (Kohler et al., 2011). To verify that the insertion in the *iolA* gene is indeed responsible for the growth phenotype, a complementation experiment was performed. A 1600 bp fragment containing the wild type *iolA* gene was cloned into the broad host range expression vector pTE3 and conjugated into the *iolA* mutant (see Material and Methods). Genes cloned into pTE3 are constitutively expressed in *S. meliloti* (Egelhoff et al., 1985). To confirm the presence of the wild-type and the mutated gene, PCR was performed. Both genes were present in four different complemented mutants (Fig. 16).

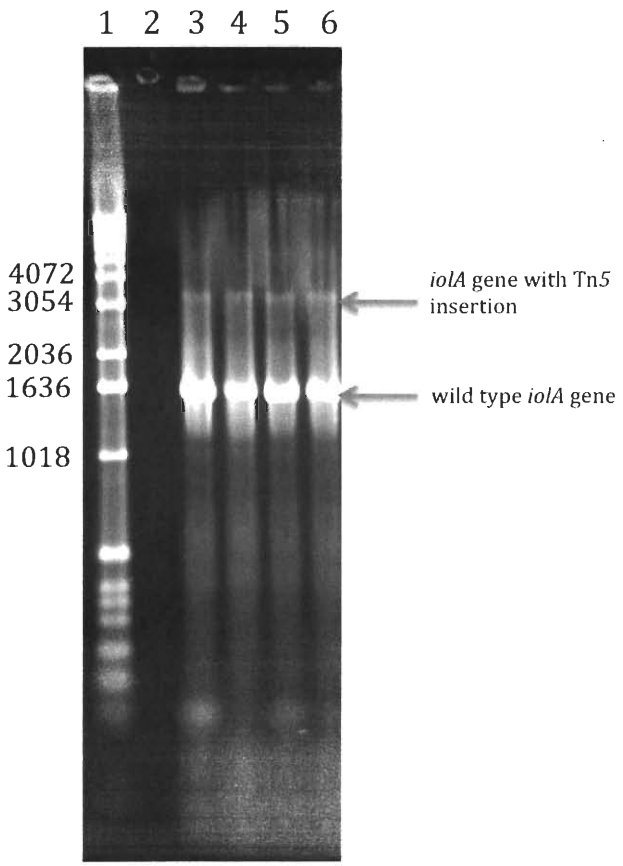

Figure 16: Confirmation of the complemented mutant WIOLA/pIolA by PCR. Photograph of an agarose gel after electrophoresis and ethidium bromide staining. Primers used were IolA forward and IolA reverse (Table 3).

Lane 1: 1kb extension ladder from NEB. Lane 2: empty. Lane 3, 4, 5 and 6: Four different complemented mutants containing a copy of the *iolA* gene with mini-Tn*5* insertion around 3500 bp and the 1450 bp wild type gene as templates.

The wild-type strain 2011, the WIOLA mutant, the complemented WIOLA/pIolA mutant and WIOLA/pTE3 mutant with the empty vector as control were subjected to growth studies with either 0.2% glycerol, *myo*-inositol, or valine as the sole carbon source. The wild type 2011 reached an $OD_{600} \approx 2.8$, whereas the WIOLA/pIolA reached an $OD_{600} \approx 2.5$ with 0.2% glycerol as the sole carbon sources. Interestingly, growth delayed was observed with the WIOLA mutant as well as the complemented WIOLA/pIolA mutant (Fig. 17A). Both the WIOLA and the WIOLA/pTE3 mutants reached an OD_{600} of 2.0 and 1.8 respectively.

As shown in Figure 17B, the wild type strain 2011 reached an $OD_{600} \approx 2.5$ with *myo*-inositol as the sole carbon source. Also, the complemented WIOLA/pIolA mutant reached an $OD_{600} \approx 2.4$ when *myo*-inositol was offered as the sole carbon source. The WIOLA mutant and the WIOLA/pTE3 mutant with the empty vector only reached an $OD_{600} \approx 0.1$ when *myo*-inositol was provided as the sole carbon source, therefore they did not show any real growth.

As shown in Figure 17C, the wild type 2011 reached an $OD_{600} \approx 1$ with 0.2% valine as the sole carbon source. The WIOLA/pIolA complemented mutant reached an $OD_{600} \approx 0.85$ with valine as the sole carbon source that is comparable to the wild type. Both the WIOLA and the WIOLA/pTE3 mutants did not grow; they reached an $OD_{600} \approx 0.1$ when valine was offered as the sole carbon source. The WIOLA and the WIOLA/pTE3 mutants showed the expected growth deficient phenotype with both *myo*-inositol and valine as sole carbon sources, and the phenotype of the

complemented mutant showed that it was indeed the *iolA* gene and not another secondary mutation in the genome that caused the phenotype.

A.

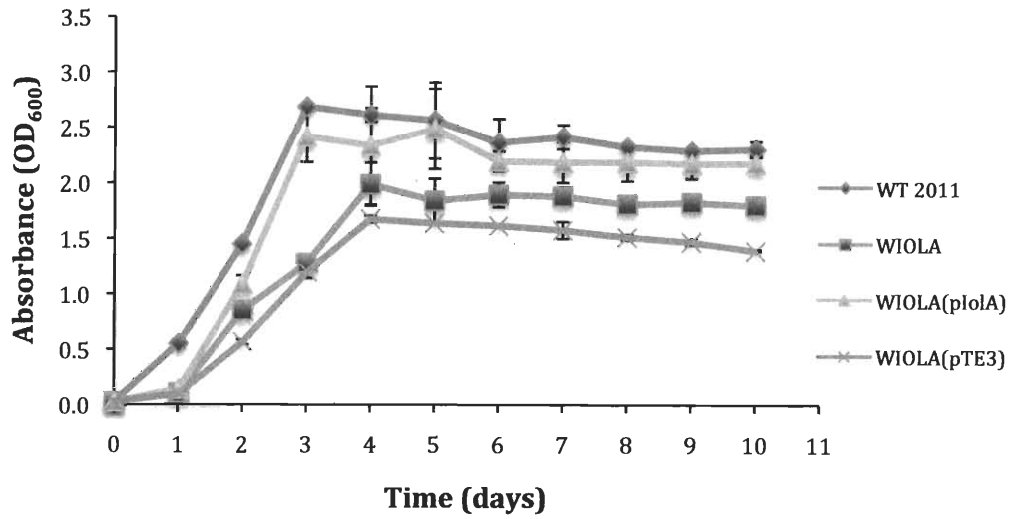

B.

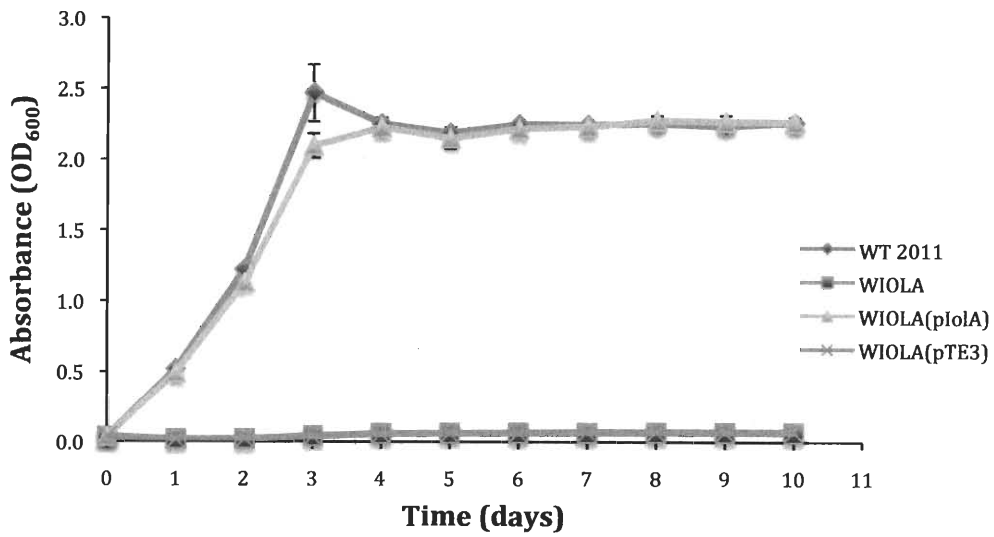

C.

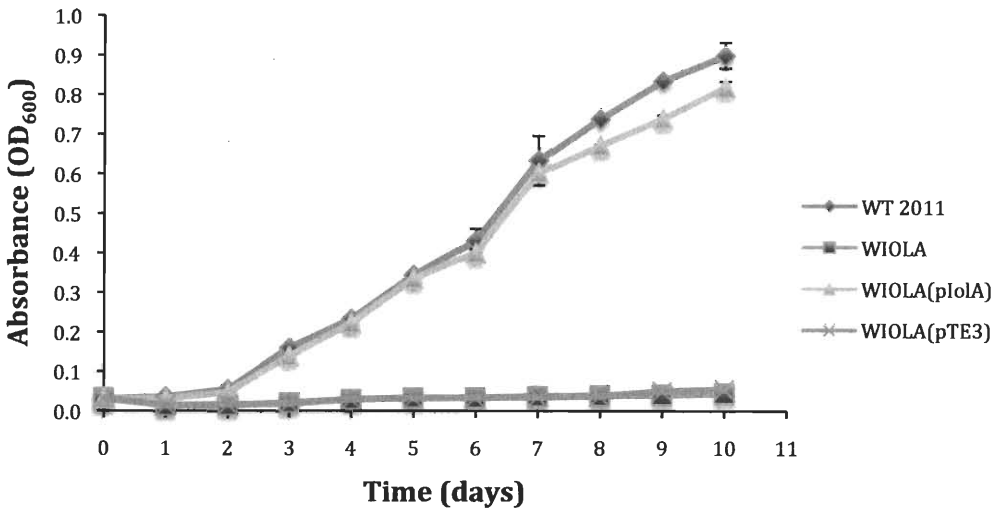

Figure 17: Growth of *S. meliloti* WT 2011 and mutants in minimal media containing either 0.2% glycerol (A), 0.2% *myo*-inositol (B), or 0.2% valine (C) as the sole carbon source. Growth was measured spectrophotometrically at 600 nm in for 10 days. This experiment was performed in triplicate. Error bars denote the standard error of the mean (SEM).

Regulation of *iolA* gene expression

The *iolA* mutant contains a mini-Tn5 insertion with a promoterless *gusA* reporter gene (Pobigaylo et al., 2006). Due to the lack of its own promoter, the *gusA* gene will only be transcribed if oriented in the same direction as the gene it has inserted into. If the host gene is being actively transcribed, the correctly oriented *gusA* gene is an ideal reporter to measure the gene expression. The *gusA* gene encodes the β-glucuronidase. This specific enzyme cleaves 4-nitrophenyl-β-D-glucuronide (PNPG), yielding β-D-glucuronic acid and *p*-nitrophenol, the latter being yellow and measurable spectrophotometrically at 405 nm.

The WIOLA mutant with the empty pTE3 vector and the complemented WIOLA/pIolA mutant were grown in minimal medium containing either 0.2% glycerol or, for induction, in medium containing 0.1% glycerol plus 0.1% *myo*-inositol as carbon sources. The *iolA* mutant with the empty vector displayed high β-glucuronidase activity (383 nmol min^{-1} OD_{600} $unit^{-1}$) as compared to the complemented mutant WIOLA/pIolA (10 nmol min^{-1} OD_{600} $unit^{-1}$). The β-glucuronidase activity of the *iolA* mutant was around five and a half times higher when it was induced with *myo*-inositol (2096 nmol min^{-1} OD_{600} $unit^{-1}$), whereas the complemented WIOLA/pIolA mutant displayed only low β-glucuronidase activity with 21 nmol min^{-1} OD_{600} $unit^{-1}$, when induced with *myo*-inositol.

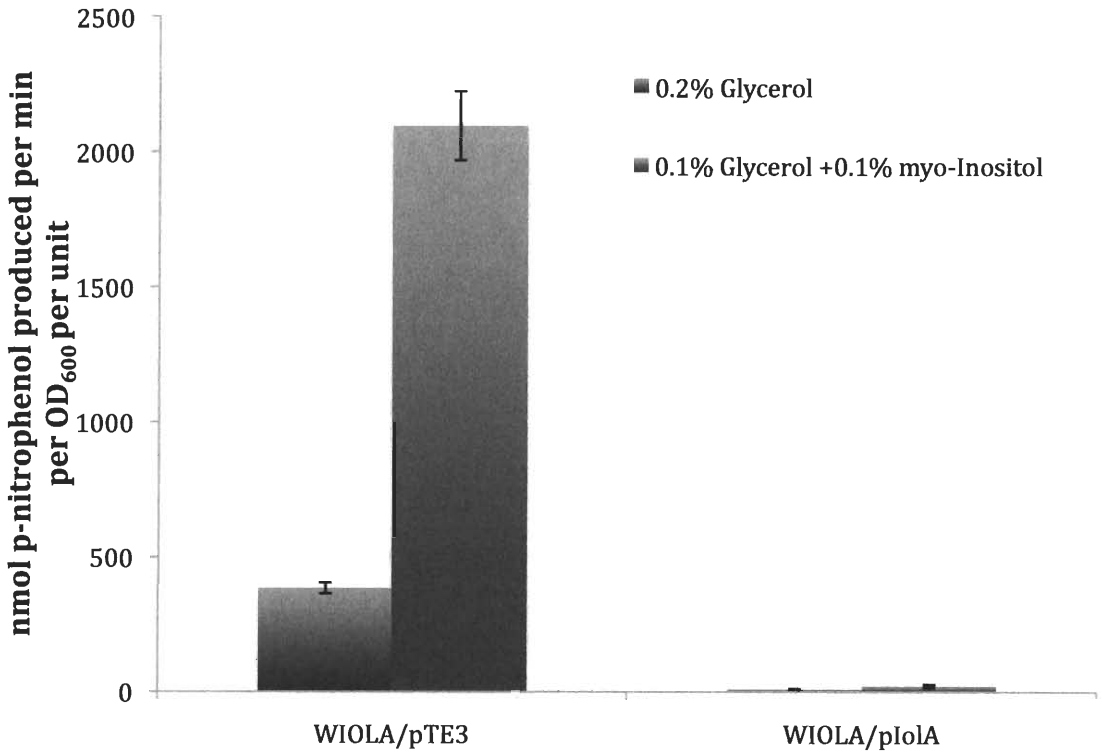

Figure 18: β-glucuronidase activity of the *iolA::gusA* fusion. The *iolA* mutant was grown in minimal media with 0.2% glycerol or 0.1% glycerol plus 0.1% *myo*-inositol as carbon sources. The reaction rate is expressed in nmol *p*-nitrophenol produced per minute per OD_{600}. The experiment was performed three times.

Regulation of the *myo*-inositol dehydrogenase activity

Not only the expression of the *iolA* gene, but also the *myo*-inositol dehydrogenase activity of the WIOLA mutant had been found to be much higher as compared to the wild-type *S. meliloti* strain (Kohler et al., 2010). The increased activity could be due to inducer accumulation of the pathway intermediate, 2-deoxy-5-keto-D-gluconic acid 6-phosphate (DKGP). To prove that the high level of the *myo*-inositol dehydrogenase activity was due to the non-functional *iolA* gene, the *iolA* mutant and the complemented mutant were subjected to a *myo*-inositol dehydrogenase assay. The wild-type strain and the complemented *iolA* mutant displayed *myo*-inositol dehydrogenase activities of 112 and 128 nmol NAD reduced min^{-1} mg $protein^{-1}$, respectively (Fig. 19). This finding is another hint that the increase of *myo*-inositol dehydrogenase activity could be due to inducer accumulation. The non-complemented *iolA* mutant showed a much higher *myo*-inositol dehydrogenase activity with 484 nmol NAD reduced min^{-1} mg $protein^{-1}$. When providing the wild-type *iolA* gene in *trans*, the final step of the inositol catabolism pathway is completed and will no longer cause the accumulation of inducers and the complemented mutant behaves like the wild type (Fig. 18).

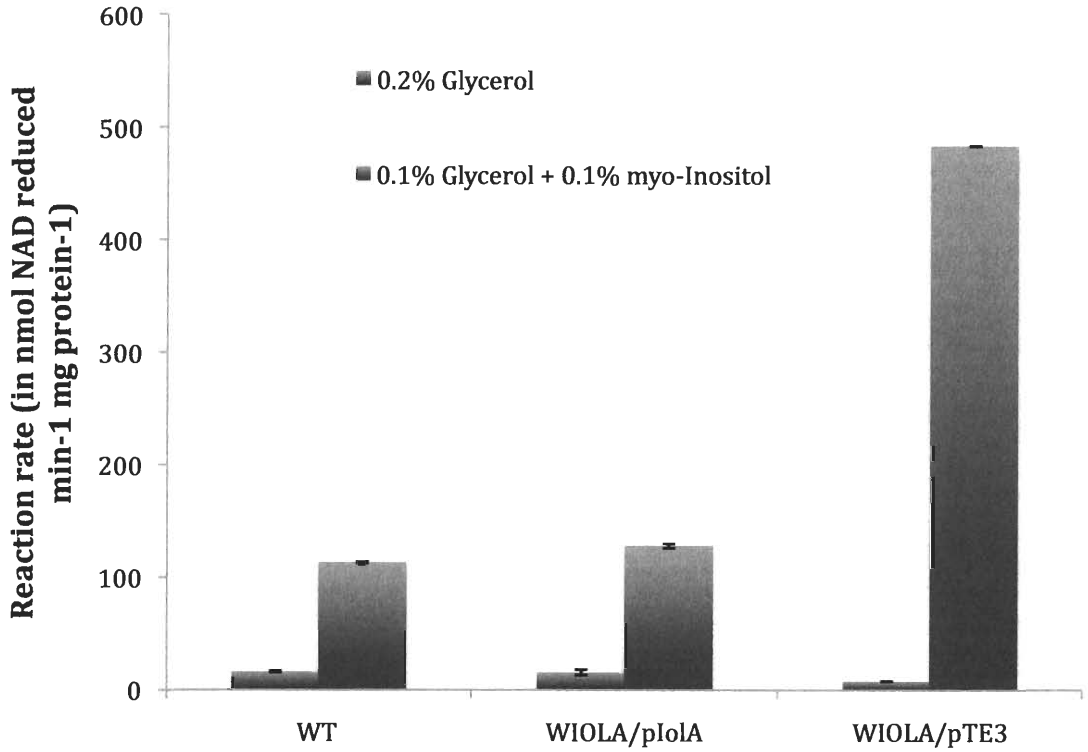

Figure 19: NAD(H)-dependent *myo*-inositol dehydrogenase assay with crude cell extracts of *S. meliloti* wild-type and mutant strains grown in minimal medium containing either 0.2% glycerol or 0.1% *myo*-inositol plus 0.1% glycerol. The reaction rate is expressed in nmol NAD^+ reduced per minute per mg protein. Bars represent the average of two independent experiments. Error bars denote the standard error of the mean (SEM).

CHAPTER 4

DISCUSSION

This thesis describes experiments designed to test three hypotheses, all of them related to the transport and catabolism of inositols in the bacterial legume symbiont *S. meliloti*. The first hypothesis was that the *SMb20072* gene product plays a role in the transport of inositols into the cytoplasm of *S. meliloti*. The second hypothesis was that the *iolI* gene product is essential for D-*chiro*-inositol metabolism of *S. meliloti*. The third hypothesis was that the *iolA* gene product plays a role in inositol catabolism as well as valine degradation of *S. meliloti*. In fact, the evidence obtained through the experiments described in this thesis supports all of these hypotheses.

Role of the *SMb20072* gene encoding a periplasmic binding protein

First, the role of the *ibpA* gene will be discussed. Previously, it was shown that the *ibpA-iatA-iatP* operon functions as a major inositol transporter in *S. meliloti* (Boutte et al., 2008; Thwaites, 2013). The *ibpA* gene encodes a periplasmic binding protein and together with the *iatA,* and *iatP* gene products constitutes an ABC transporter (Fig. 20). When the *ibpA* gene was disrupted by a mini-Tn*5* insertion, the initial growth of the mutant was delayed with *myo*-inositol as the sole carbon source. The delayed phenotype led to the conclusion that there could be a second transporter in *S. meliloti*. In *S. enterica* serovar typhimurium and *B. subtilis* both primary and secondary transporters have been found (Kröger et al., 2010; Yoshida et al., 2002).

The analysis of the genome of *S. meliloti* revealed that besides the *ibpA* gene, *S. meliloti* contains another gene encoding a periplasmic binding protein, *SMb20072*, which we later called *ibpB*. In order to characterize the role of the second putative inositol periplasmic binding protein, a single and a double mutant with insertions in the *ibpA* and *ibpB* genes were constructed in this thesis.

The initial growth of the single *ibpB* mutant with *myo*- and D-*chiro*-inositol was delayed. The double mutant *ibpAibpB* was found to be unable to grow with *myo*-inositol, D-*chiro*-inositol or pinitol as the sole carbon source, suggesting that the *ibpA* and the *ibpB* gene are indeed both responsible for the transport of inositol compounds in *S. meliloti*. The proposed inositol transport pathway in *S. meliloti* is illustrated in Fig. 20. The *ibpA* mutant has a more drastic phenotype than the *ibpB* mutant. Therefore, we suggest that the IbpA functions as the major periplasmic binding protein whereas the IbpB functions as the minor periplasmic binding protein of *S. meliloti*. At this point, we are still unable to find a second putative permease component as well as an ATP-binding cassette (Fig. 20), if they exist.

Future directions for the work on inositol transport in *S. meliloti* includes constructing mutants in the *iatA* and *iatP* genes which encode the permease component and the ATP-binding cassette, respectively (Fig. 20) to show a clearer picture of how inositols are transported into rhizobial cells. Constructing these mutants would allow us to improve the understanding of the inositol transport in *S. meliloti*.

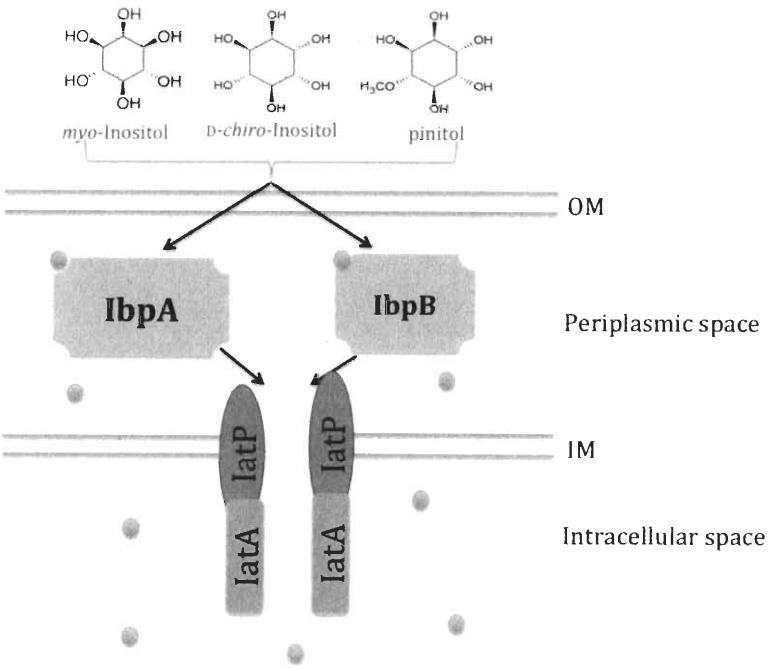

Figure 20: Schematic drawing of the putative ABC transporter encoded by the *ibpA, iatA, iatP* genes as well as the second periplasmic-binding protein, *ibpB*. OM indicates outer membrane, whereas IM indicates inner membrane.

Role of the *SMb20711* gene encoding an inosose isomerase

The second part of this discussion will deal with D-*chiro*-inositol catabolism after D-*chiro*-inositol has been transported into the cell. The *ioll* gene in *B. subtilis* has been found to be essential for D-*chiro*-inositol catabolism (Yoshida et al., 2006). In *B. subtilis*, the *ioll* gene encodes an inosose isomerase that is responsible for converting 1-keto-D-*chiro*-inositol to 2-keto-*myo*-inositol (Fig. 21). By analyzing the *S. meliloti* genome with the KEGG database, it was found that the *SMb20711* gene, which encodes a sugar epimerase that might have the same function as the *ioll* gene in *B. subtilis*. In fact, the *SMb20711* gene product of *S. meliloti* and the *ioll* gene product of *B. subtilis* share 45% similar amino acid residues and only 21% amino acid residues are identical. Regardless of the low identity, we decided to further study the function of the *SMb20711* gene in *S. meliloti*.

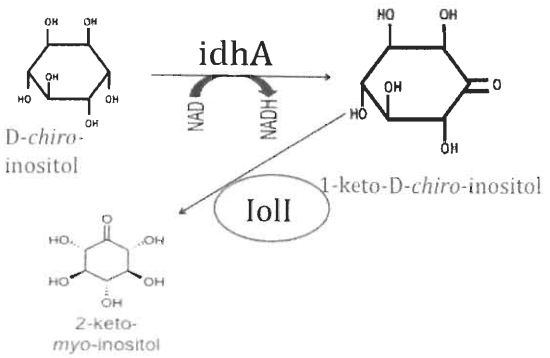

Figure 21: Function of the *ioll* gene in *S. meliloti* in D-*chiro*-inositol catabolism.

In this thesis, an *S. meliloti* mutant with an insertion in the *SMb20711* gene was constructed to characterize its role in D-*chiro*-inositol catabolism. The *SMb20711* mutant was unable to grow with D-*chiro*-inositol as the sole carbon source (Fig. 14B). This result indicates that the *SMb20711* gene is essential for D-*chiro*-inositol catabolism and we called it *ioll*. Interestingly, when *myo*-inositol and pinitol were offered as sole carbon sources, the *ioll* mutant was able to grow, but the growth was less than the growth of the *S. meliloti* 2011 wild-type strain (Fig. 14 C, D). These data suggest that the *SMb20711* gene may also play a minor role in *myo*-inositol and pinitol metabolism.

Nevertheless, the *ioll* gene is located directly upstream of the *ibpA-iatA-iatP* genes encoding the major inositol transporter (Fig. 6). An alternative explanation for our result is that the mutation in the *SMb20711* gene has a polar effect on the downstream located *ibpA-iatA-iatP* genes that might cause the transport genes to be not fully functional.

The *iolA* gene product has multiple roles

The third part of this discussion considers the role of the *iolA* gene. The *iolA* gene encodes a methyl malonate semialdehyde dehydrogenase that is the last enzyme in the proposed inositol catabolism pathway. It was shown to be required for inositol catabolism in *B. subtilis* (Yoshida et al., 2008) and *S. meliloti* (Kohler et al., 2010). The *iolA* gene was also shown to be essential for valine catabolism in *Pseudomonas spp.* (Bannerjee et al., 1970; Puukka et al., 1973; and Steele et al., 1992), as well as in *S. meliloti* (Kohler et al., 2011). In this thesis, I showed that the *S. meliloti iolA* mutant could be complemented with the *iolA* gene, thereby confirming that the phenotype of the *iolA* mutant is indeed due to the transposon insertion in the *iolA* gene and not due to a second site mutation somewhere else in the genome.

In summary, in this thesis I characterized three genes that are necessary for the transport and catabolism of inositol and its derivatives in *S. meliloti*. The first gene is the *SMb20072* (*ibpB)* gene, which encodes a periplasmic binding protein. It was demonstrated that this protein plays a role in the transport of *myo-* and D-*chiro*-inositol as well as of the inositol derivative pinitol. The second gene is the *SMb20711* (*iolI*) gene, which encodes an inosose isomerase. It was demonstrated that this gene plays an essential role in D-*chiro*-inositol catabolism. Last but not least, this work proved that the insertion in the *iolA* gene was responsible for the observed phenotype (Kohler et al., 2011). The results presented in this thesis help to refine the knowledge about the inositol catabolism pathway in *S. meliloti.*

REFERENCES

Anderson, W. A., and B. Magasanik. (1971). The cyclitols. *pp* 519-579. *In* W. Pigman and D. Horton (ed), The Carbohydrates, 2nd ed, Vol. 1A. Academic Press, New York.

Anderson, W. A., & Magasanik, B. (1971a). The pathway of *myo*-inositol degradation in *Aerobacter aerogenes* conversion of 2-deoxy-5-keto-D-gluconic acid to glycolytic intermediates. Journal of Biological Chemistry **246**:5662-5675.

Anderson, W. A., and B. Magasanik. (1971b). The pathway of *myo*-inositol degradation in *Aerobacter aerogenes* – Identification of the intermediate 2-deoxy-5-keto-D-gluconic acid. Journal of Biological Chemistry **246:**5653-5661.

Bannerjee. D., L. E. Sanders, and J. R. Sokatch. (1970). Properties of purified methylmalonate semialdehyde dehydrogenase of *Pseudomonas aeruginosa.* Journal of Biological Chemistry **245:**1828-1835.

Bauer, W. D. (1981). Infection of legumes by rhizobia. Annual Review of Plant Physiology **32**:407-449.

Berman, T., and B. Magasanik. (1966a). The pathway of *myo*-inositol degradation in *Aerobacter aerogenes* – Dehydrogenation and dehydration. Journal of Biological Chemistry **241:**800-806.

Berman, T., and B. Magasanik. (1966b). The pathway of *myo*-inositol degradation in *Aerobacter aerogenes* – Ring scission. Journal of Biological Chemistry **241:**807-812.

Borges, N., Gonçalves, L. G., Rodrigues, M. V., Siopa, F., Ventura, R., Maycock, C., and H. Santos. (2006). Biosynthetic pathways of inositol and glycerol phosphodiesters used by the hyperthermophile Archaeoglobus fulgidus in stress adaptation. Journal of Bacteriology **188:**8128-8135.

Boutte C., B. Srinivasan, J. Flannick, A. Novak, A. Martens, S. Batzoglou, P. Viollier, and S. Crosson. (2008). Genetic and computational identification of a conserved bacterial metabolic module. PLoS Genetics **4**:e1000310.

Bray, E. A. (1997). Plant responses to water deficit. Trends in Plant Science **2:**48-54.

Brewin, N. J., Robertson, J. G., Wood, E. A., Wells, B., Larkins, A. P., Galfra, G., and Butcher, G. W. (1985). Monoclonal antibodies to antigens in the peribacteroid membrane from *Rhizobium*-induced root nodules of pea cross-react with plasma membranes and Golgi bodies. EMBO Journal **4:**605-611

Browning D., and S. Busby. (2003). The regulation of bacterial transcription initiation. Nature Reviews Microbiology **2:**57-65.

Cheng, Q. (2008). Perspectives in biological nitrogen fixation research. Journal of Integrated Plant Biology **50:**786-798.

Dehusses. J., and G. Reber. (1972). *myo*-Inositol transport in *Aerobacter aerogenes*. Biochemical et Biophysical Acta–Biomembranes **274:**598-605.

Dehusses. J., and G. Reber. (1977). *myo*-Inositol transport in *Klebsiella aerogenes. scyllo*-Inositol, a non-metabolizable substrate for the study of the *myo*-inositol transport system. European Journal of Biochemistry **72:**87-91.

Dehusses. J., and G. Reber. (1977). Asymmetry of the *myo*-inositol transport system in *Klebsiella aerogenes* is necessary to create the asymmetry of the transport system. European Journal of Biochemistry/ FEBS **72:**101-106.

Dehusses. J., and M. Belet. (1984). Purification and properties of the *myo*-inositol-binding protein from a *Pseudomonas spp.* Journal of Bacteriology **159:**179-183.

Dehusses, J. P. (1985). *myo*-Inositol transport in bacteria: H^+ symport and periplasmic binding protein dependence. Annals of the New York Academy of Science **456:**351-360.

Do, G. M., Choi, M. S., Kim, H. J., Woo, M. N., Lee, M. K., and Jeon, S. M. (2008). Soy pinitol acts partly as an insulin sensitizer or insulin mediator in 3T3-L1 preadipocytes. Genes & Nutrition **2**:359-364.

Egelhoff, T. T., and S. R. Long (1985). *Rhizobium meliloti* nodulation genes: identification of *nodDABC* gene products, purification of NodA protein, and expression of *nodA* in *Rhizobium meliloti*. Journal of Bacteriology **164:**591-599.

Ehrhardt, D. W., Wais, R., and Long, S. R. (1996). Calcium spiking in plant root hairs responding to Rhizobium nodulation signals. Cell **85**:673-681.

Fenili, D., Brown, M., Rappaport, R., and J. McLaurin. (2007). Properties of *scyllo*-inositol as a therapeutic treatment of AD-like pathology. Journal of Molecular Medicine **85:**603-611.

Fenili, D., Ma, K., and J. McLaurin. (2010). *scyllo*-Inositol: A potential therapeutic for Alzheimer's disease. In A. Martinez (Ed), Emerging Drugs and Targets for Alzheimer's Disease **1**:94-116

Finan, T. M., Hirsch, A. M., Leigh, J. A., Johansen, E., Kuldau, G. A., Deegan, S., and Signer, E. R. (1985). Symbiotic mutants of Rhizobium meliloti that uncouple plant from bacterial differentiation. Cell **40**:869-877.

Finan, T. M., Kunkel, B., De Vos, G. F., and E. R. Singer. (1986). Second symbiotic megaplasmid in *Rhizobium meliloti* carrying exopolysaccharide and thiamine synthesis genes. Journal of Bacteriology **167**:66-72.

Fischer, M., Zhang, Q. Y., Hubbard, R. E., and Thomas., G. H. (2010). Caught in TRAP: substrate-binding proteins in secondary transport. Trends in Microbiology **18**:471-478

Fry, J., M. Wood, and P. Poole. (2001). Investigation of *myo*-inositol catabolism in *Rhizobium leguminosarum bv. viciae* and its effect on nodulation competitiveness. Molecular Plant-Microbe Interactions **14**:1016-1025.

Galbraith, M., Feng, S., Borneman, J., Triplett, E., De Bruijn, F., and S. Rossbach. (1998). A functional *myo*-inositol catabolism pathway is

essential for rhizopine utilization by *Sinorhizobium meliloti*. Microbiology **144:**2915-2924.

Galibert, F., Finan, T. M., Long, S. R., Pühler, A., Abola, P., Ampe, F., and M. Vandenbol. (2001). The composite genome of the legume symbiont *Sinorhizobium meliloti*. Science **293:**668-672.

Halverson, L. J., and Stacey, G. (1986). Signal exchange in plant-microbe interactions. Microbiological Reviews **50**:193.

Herrou, J., and S. Crosson (2013). *myo*-Inositol and D-ribose ligand discrimination in an ABC periplasmic binding protein. Journal of Bacteriology **195**:2379-2388.

Jiang, G., Krishnan, A. H., Kim, Y. W., Wacek, T. J., and H. B. Krishnan. (2001). A functional *myo*-inositol dehydrogenase gene is required for efficient nitrogen fixation and competitiveness of *Sinorhizobium fredii* USDA191 to nodulate soybean (glycine max [L.] merr.). Journal of Bacteriology **183:**2595-2604.

Jones K., H. Kobayashi, B. Davies, M. Taga, and G. Walker. (2007) How rhizobial symbionts invade plants: the *Sinorhizobium-Medicago* model. Nature Reviews Microbiology **5**:619-633.

Kawsar, H. I., K. Ohtani, K., Okumura, H. Hayashi, and T. Shimizu. (2004). Organization and transcriptional regulation of *myo*-inositol operon in *Clostridium perfringens.* FEMS Microbiology Letter **235**:289-295.

Kim, J. I., K., J. C., Kang, M. J., Lee, M. S., Kim, J. J., and I. J. Cha. (2005). Effects of pinitol isolated from soybeans on glycaemic control and cardiovascular risk factors in Korean patients with type II diabetes mellitus: A randomized controlled study. European Journal of Clinical Nutrition **59:**456-458.

Kim, M. J., Yoo, K. H., Kim, J. H., Seo, Y. T., Ha, B. W., Kho, J. H., and Chung, C. H. (2007). Effect of pinitol on glucose metabolism and adipocytokines in uncontrolled type 2 diabetes. Diabetes Research and Clinical Practice **77**:S247-S251.

Kohler P., J. Zheng, E. Schoffers, and S. Rossbach. (2010). Inositol catabolism, a key pathway in *Sinorhizobium meliloti* for competitive host nodulation. Applied and Environmental Microbiology **76:**7972-7980.

Kohler P., E. L. Choong, and S. Rossbach. (2011). The RpiR-like repressor IolR regulates inositol catabolism in *Sinorhizobium meliloti.* Journal of Bacteriology **193:**5155-5163.

Kröger C., and T. M. Fuchs. (2009). Characterization of the *myo*-inositol utilization island of *Salmonella enterica* serovar Typhimurium. Journal of Bacteriology **191:**545-554.

Kröger C., J. Stolz, and T. M. Fuchs. (2010). *myo*-Inositol transport by *Salmonella enterica* serovar Typhimurium. Microbiology **156:**128-138.

Larner, J. 2002. D-*chiro*-Inositol – its functional role in insulin action and its deficit in insulin resistance. Experimental Diabetes Research **3:**47-60.

Larner, J., Brautigan, D. L., and M. O. Thorner. (2010). D-*chiro*-Inositol glycans in insulin signaling and insulin resistance. Molecular Medicine **16:**543-552.

Leyn, S. A., M. D. Kazanov, N. V. Sernova, E. O. Ermakova, P. S. Novichkov, and D. A. Rodionov. (2013). Genomic reconstruction of the transcriptional regulatory network in *Bacillus subtilis*. Journal of Bacteriology **195**:2463-2473.

Long, S. R. (1989). *Rhizobium*-legume nodulation: life together in the underground. Cell **56**:203-214.

Long, S. R. (1996). *Rhizobium* symbiosis: Nod factors in perspective. Plant Cell **8:**1885-1898.

Martin, D. D., Ciulla, R. A., & Roberts, M. F. (1999). Osmoadaptation in Archaea. Applied and Environmental Microbiology **65**: 1815-1825.

Mauchline T., J. Fowler, A. East, A. Sartor, R. Zaheer, A. Hosie, P. Poole, and T. Finan. (2006). Mapping the *Sinorhizobium meliloti* 1021 solute-binding protein-dependent transportome. PNAS **103:**17933-17938.

Meade, H. M., S. R. Long, G. B. Ruvkun, S. E. Brown, and F. M. Ausubel. (1982). Physical and genetic characterization of symbiotic and auxotrophic mutants of *Rhizobium meliloti* induced by transposon Tn*5* mutagenesis. Journal of Bacteriology **149:**114-122.

Michell, R. H. (2008). Inositol derivatives: evolution and functions. Nature Reviews Molecular Cell Biology **9**:151-161.

Morinaga, T., H. Aishida, and K. Yoshida. (2010). Identification of two *scyllo*-inositol dehydrogenases in *Bacillus subtilis.* Microbiology **156**:1538-1546.

Morinaga, T., T. Matsuse, H. Aishida, and K. Yoshida. (2010). Differential substrate specificity of two inositol transporters of *Bacillus subtilis.* Bioscience, Biotechnology and Biochemistry **74:**1312-1314.

Morinaga T., M. Yamaguchi, Y. Makino, H. Nanamiya, K. Takashi, H. Yoshikawa, F. Kawamura, H. Ashida, and K. Yoshida. (2006). Functional *myo*-inositol catabolic genes of *Bacillus subtilis* Natto are involved in depletion of pinitol in Natto (fermented soybean). Bioscience, Biotechnology, and Biochemistry **70:**1913-1920.

Newcomb, W., Sippell, D., and Peterson, R. L. (1979). The early morphogenesis of *Glycine max* and *Pisum sativum* root nodules. Canadian Journal of Botany **57**:2603-2616.

Nguyen, A., & Lamant, A. (1988). Pinitol and *myo*-inositol accumulation in water-stressed seedlings of maritime pine. Phytochemistry **27**:3423-3427.

Pobigaylo, N., D. Wetter, S. Szymczak, U. Schiller, S. Kurtz, F. Meyer, T. W. Nattkemper, and A. Becker. (2006). Construction of a large signature-tagged mini-*Tn5* transposon library and its application to mutagenesis of *Sinorhizobium meliloti.* Applied and Environmental Microbiology **72:**4239-4337.

Poole, P. S., A. Blyth, C. J. Reid, and K. Walters. (1994). *myo*-Inositol catabolism and catabolite regulation in *Rhizobium leguminosarum* bv. *viciae.* Microbiology **140:**2787-2795.

Prentki, P. & Krisch, H. M. (1984). In vitro mutagenesis with a selecable DNA fragment. Gene **29:**303-313.

Puukka, M. 1973. Regulation of valine degradation in *Pseudomonas fluorescens* UK-1. Induction of enoyl coenzyme A hydratase. Acta Chemica Scandinavica **27**:718-719.

Quandt, J., and M. F. Hynes. (1993). Versatile suicide vectors, which allow directed selection for gene replacement in Gram-negative bacteria. Gene **127:**15-21.

Ramaley, R., Y. Fujita, and E. Freese. (1979). Purification and properties of *Bacillus subtilis* inositol dehydrogenase. Journal of Biological Chemistry **254**:7684-7690.

Reber, G., M. Mermod, and J. Dehusses. (1977). Transport of cyclitols by a proton symport in *Klebsiella aerogenes.* European Journal of Biochemistry **72**:93-99.

Reber, G., Belet, M., and J. Dehusses. (1977). *myo*-Inositol transport system in *Pseudomonas putida.* Journal of Bacteriology **131**: 872-875.

Richardson, A. E., and P. A. Hadobas. (1997). Soil isolates of *Pseudomonas spp.* that utilize inositol phosphates. Canadian Journal of Microbiology **43**:509-516.

Sambrook, J., Fritscg, E. F., and T. Maniatis. (1989). Molecular cloning: A laboratory manual (2nd Ed.). New York, NY. Cold Spring Harbor Laboratory Press.

Simon, R., Priefer, U. and Pühler, A. (1983). A broad host range mobilization system for *in vivo* genetic engineering: transposon mutagenesis in Gram-negative bacteria. Nature Biotechnology **1:**784-790.

Steele, M. I., D. Lorenz, K. Hatter, A. Park, and J. R. Sokatch. (1992). Characterization of the *mmsAB* operon of *Pseudomonas aeruginosa* PAO encoding methylmalonate-semialdehyde dehydrogenase and 3-hydroxyisobutyrate dehydrogenase. Journal of Biological Chemistry **267**:13585-13592.

Sundaram, T. K. (1972). *myo*-Inositol catabolism in *Salmonella typhimurium:* Enzyme repression dependent on growth history of organism. Journal of General Microbiology **73**:209-219.

Talfournier F., C. Stines-Chaumeil, and G. Branlant. (2011). Methylmalonate-semialdehyde dehydrogenase from *Bacillus subtilis*: substrate specificity and coenzyme A binding. Journal of Biological Chemistry **286:**21971-21981.

Thwaites, M. (2013). Inositol transport and catabolism of inositol derivatives in *Sinorhizobium meliloti* [Thesis]. Kalamazoo: Western Michigan University.

Turgeon, B. G., and W. D. Bauer. (1985). Ultrastructure of infection-thread development during the infection of soybean by *Rhizobium japonicum*. Planta **163**:328-349.

Vandenbosch, K. A., Noel, K. D., Kaneko, Y., and E. H. Newcomb. (1985). Nodule initiation elicited by noninfective mutants of *Rhizobium phaseoli*. Journal of bacteriology **162:**950-959.

Varela-Nieto, I., Leon, Y., and H. N. Caro. (1996). Cell signaling by inositol phosphoglycans from different species. Comparative Biochemistry Physiology Part B: Biochemistry and Molecular Biology **115:**223-241.

Winnen, B., Hvorup, R. N., and M. H. Saier Jr (2003). The tripartite tricarboxylate transporter (TTT) family. Research in Microbiology, **154**:457-465.

Yoshida, K., D. Aoyama, I. Ishio, T. Shibayama, and Y. Fujita. (1997). Organization and transcription of the *myo*-inositol operon, *iol*, of *Bacillus subtilis*. Journal of Bacteriology **179:**4591-4598.

Yoshida, K., T. Shibayama, D. Aoyama, and Y. Fujita. (1999). Interaction of a repressor and its binding sites for regulation of the *Bacillus subtilis ioll* divergon. Journal of Molecular Biology **285**:917-929.

Yoshida K., Y. Yamamoto, and K. Omae, M. Yamamoto, and Y. Fujita. (2002). Identification of two *myo*-inositol transporter genes of *Bacillus subtilis*. Journal of Bacteriology **184**:983-991.

Yoshida K., M. Yamaguchi, H. Ikeda, K. Omae, K. Tsurusaki, and Y. Fujita. (2004). The fifth gene of the *iol* operon of *Bacillus subtilis, iolE,* encodes 2-keto-*myo*-inositol dehydratase. Microbiology **150:**571-580.

Yoshida, K., W. S. Kim, M. Kinehara, R. Mukai, H. Ashida, H. Ikeda, Y. Fujita, and H. B. Krishnan. (2006). Identification of a functional 2-keto-*myo*-inositol dehydratase gene of *Sinorhizobium fredii* USDA191 required for *myo*-inositol utilization. Bioscience, Biotechnology and Biochemistry **70:**2957-2964.

Yoshida K., M. Yamaguchi, T. Morinaga, M. Ikeuchi, M. Kinehara, and H. Ashida. (2006). Genetic modification of *Bacillus subtilis* for production of D-*chiro*-inositol, an investigational drug candidate for treatment of type 2 diabetes and polycystic ovary syndrome. Applied and Environmental Microbiology **72**:1310-1315.

Yoshida K., M. Yamaguchi, T. Morinaga, M. Kinehara, M. Ikeuchi, H. Ashida and Y. Fujita. (2008). *myo*-inositol catabolism in *Bacillus subtilis.* Journal of Biological Chemistry **283:**10415-10424.